

1,10-Phenanthroline and 4,5-diazafluorene ketones and their Silver(I) and Platinum(II) complexes: Synthesis and biological evaluation as antiproliferative agents

Leonardo Sandin-Mazzondo¹, Jesús M. Martínez-Ilarduya¹, Jesús A. Miguel,¹ Camino Bartolomé*¹ and Concepción Alonso*²

¹ IU CINQUIMA/Química Inorgánica, Facultad de Ciencias, Universidad de Valladolid, 47071, Valladolid (Spain);

² Departamento de Química Orgánica I, Facultad de Farmacia, Universidad del País Vasco, 01006, Vitoria-Gasteiz (Spain)

* Correspondence:

Contents

1. Ligands: NMR spectra	2
2. Ag(I) complexes: NMR spectra	5
3. Pt(II) complexes: NMR spectra	9
4. ESI-TOF mass spectra of 2Ag	15
5. Stability of complexes in DMSO	16
6. Stability of the compounds in DMSO:H ₂ O (3:1)	18
7. Crystal data and structural refinement results	22

1. Ligands: NMR spectra

1,10-phenanthroline-5,6-dione (**1**)

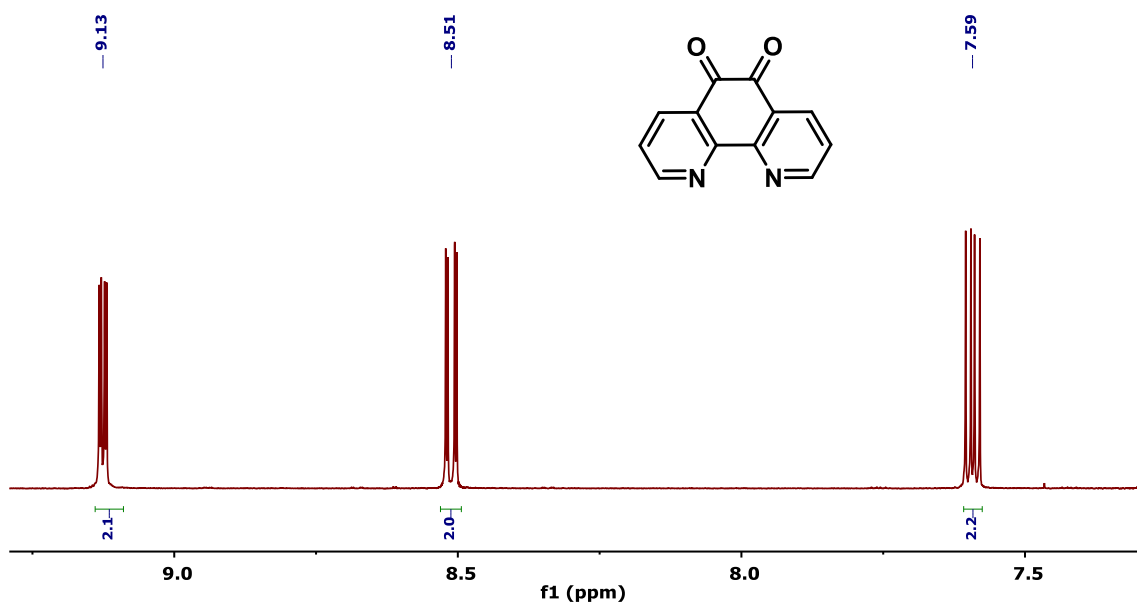


Figure S1. ¹H-NMR of **1** (CDCl₃, 298 K)

(R/S)-6-hydroxy-6-(2-oxypropyl)-1,10-phenanthroline-5(6H)-one (**2**)

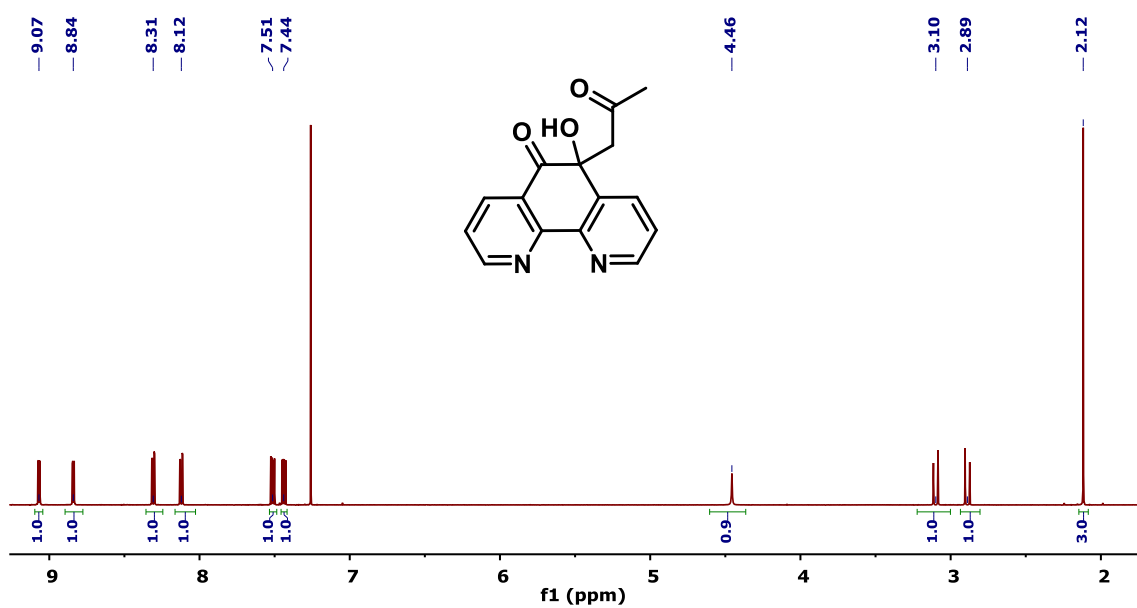


Figure S2. ¹H-NMR of **2** (CDCl₃, 298 K)

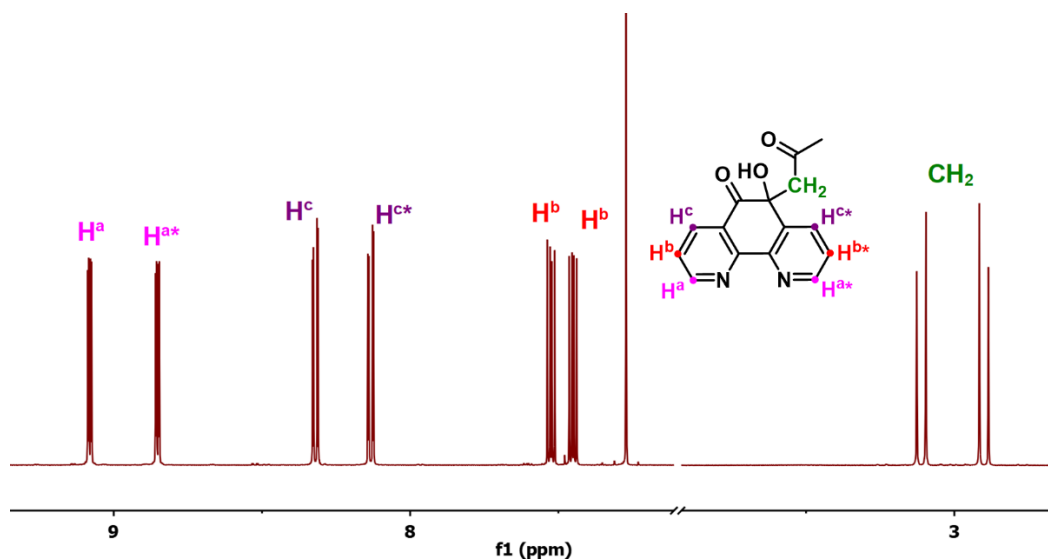


Figure S3. Aromatic and methylene ^1H -NMR signals of compound **2** (CDCl_3 , 298 K)

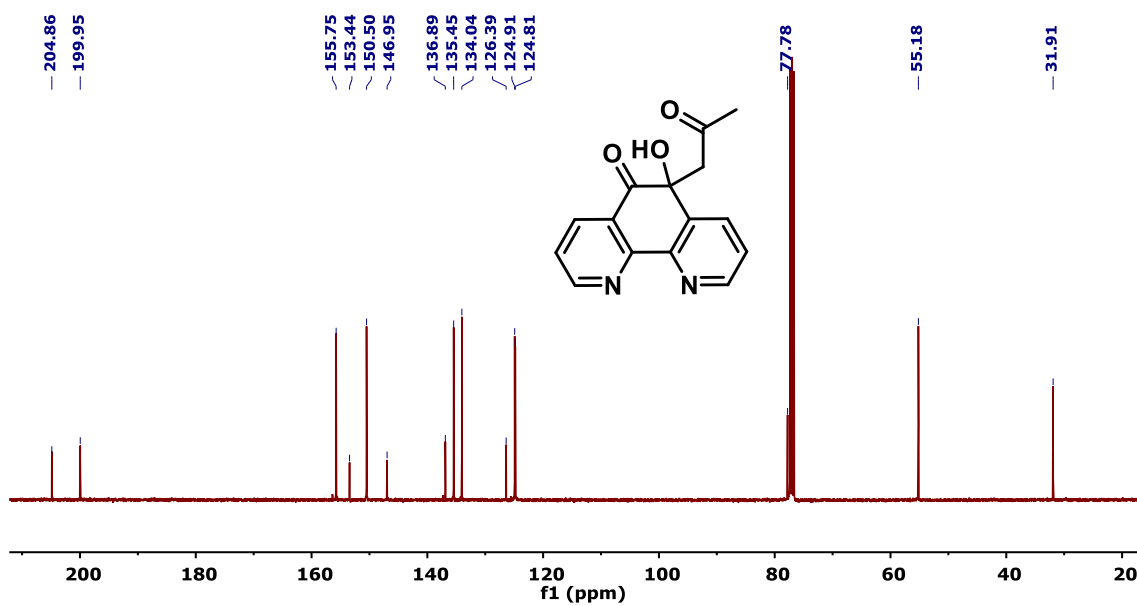


Figure S4. ^{13}C -NMR of **2** (CDCl_3 , 298 K)

4,5-diazafluoren-9-one (**3**)

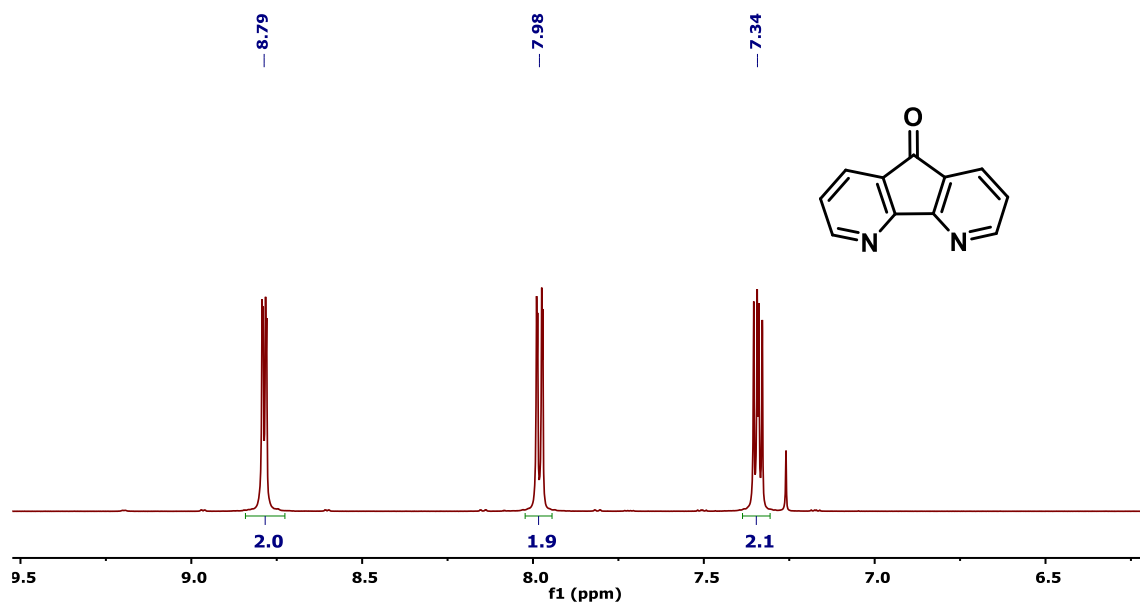


Figure S5. $^1\text{H-NMR}$ of **3** (CDCl_3 , 298 K)

9-hydroxy-9-(2-oxopropyl)-4,5-diazafluorene (**4**)

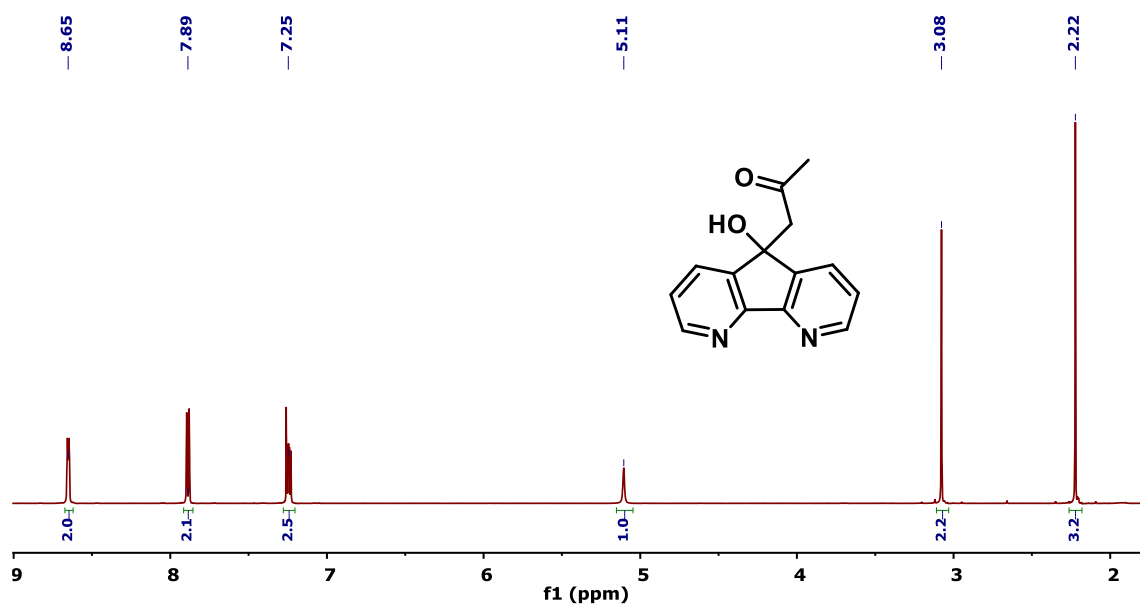


Figure S6. $^1\text{H-NMR}$ of **4** (CDCl_3 , 298 K)

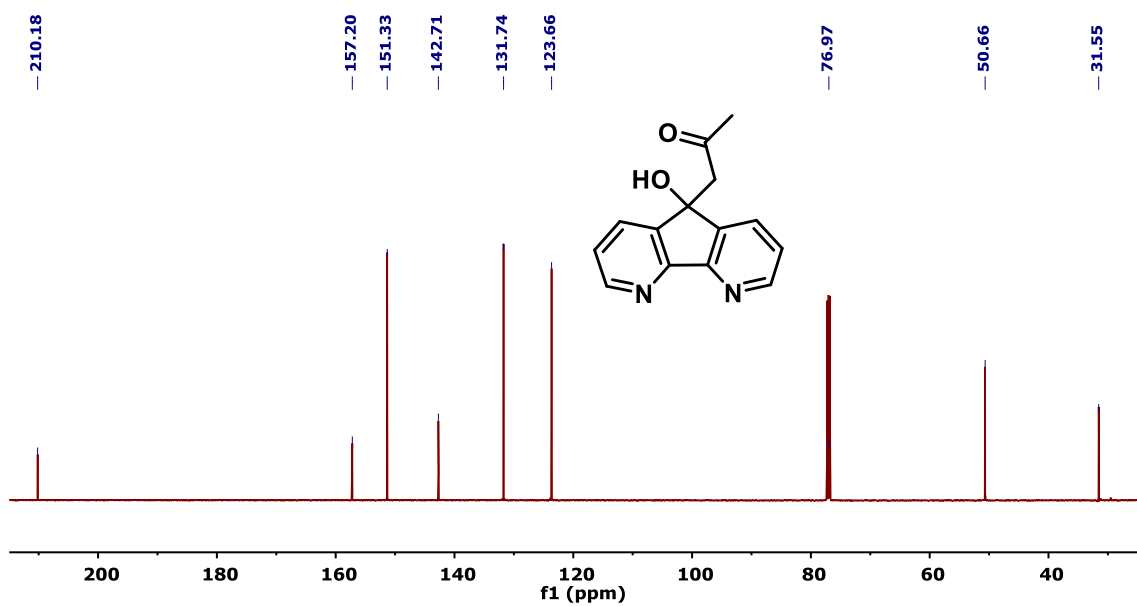


Figure S7. ^{13}C -NMR of **4** (CDCl_3 , 298 K)

2. Ag(I) Complexes: NMR spectra

[Ag(1,10-phenanthroline-5,6-dione) $_2$] NO_3 (**1Ag**)

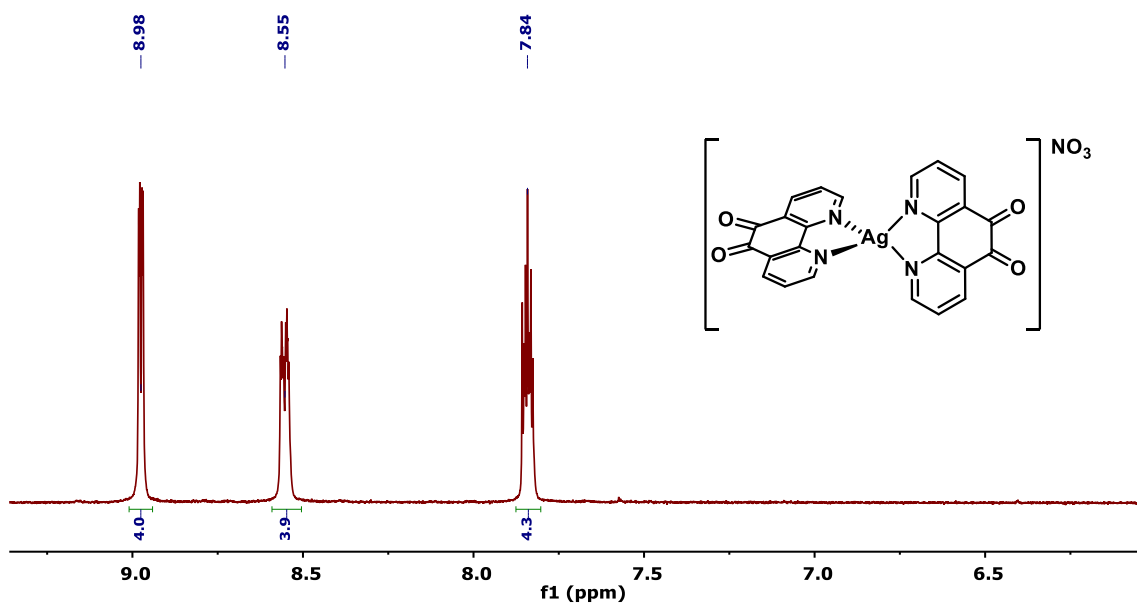


Figure S8. ^1H -NMR of **1Ag** (DMSO-d_6 , 298 K)

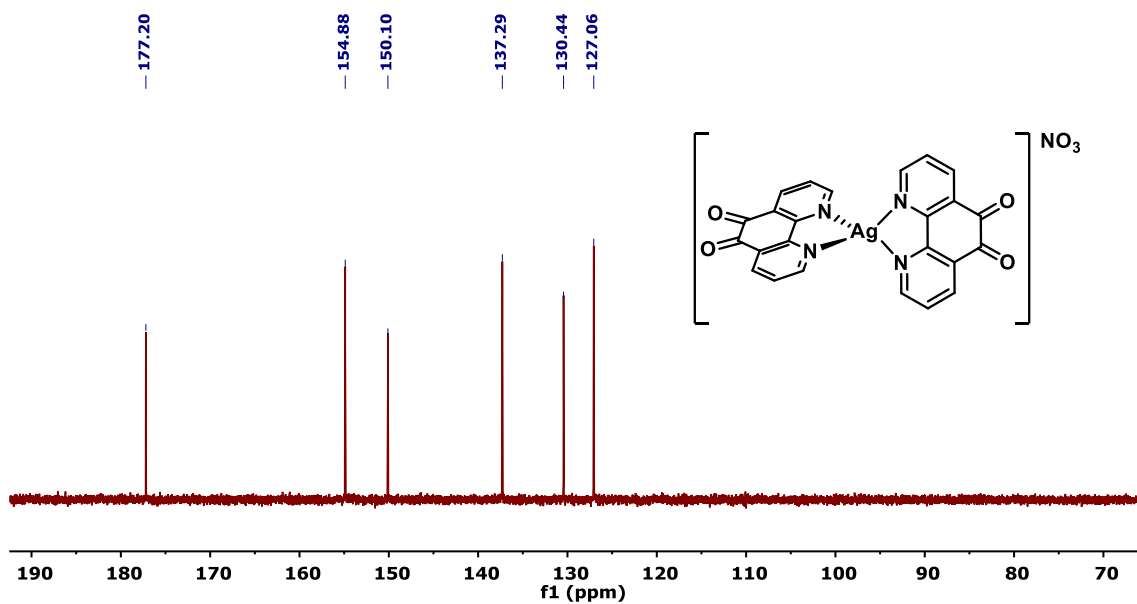


Figure S9. ^{13}C -NMR of **1Ag** (DMSO-d_6 , 298 K)

$[\text{Ag}((R/S)\text{-6-hydroxy-6-(2-oxypropyl)-1,10-phenanthroline-5(6H)-one})_2]\text{NO}_3$ (**2Ag**)

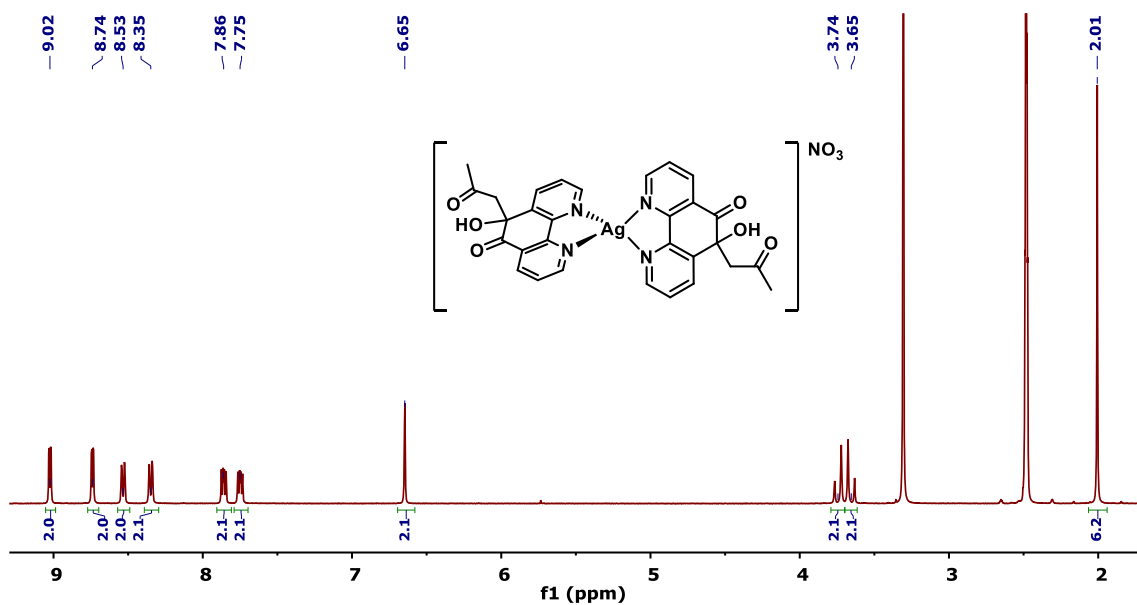


Figure S10. ^1H -NMR of **2Ag** (DMSO-d_6 , 298 K)

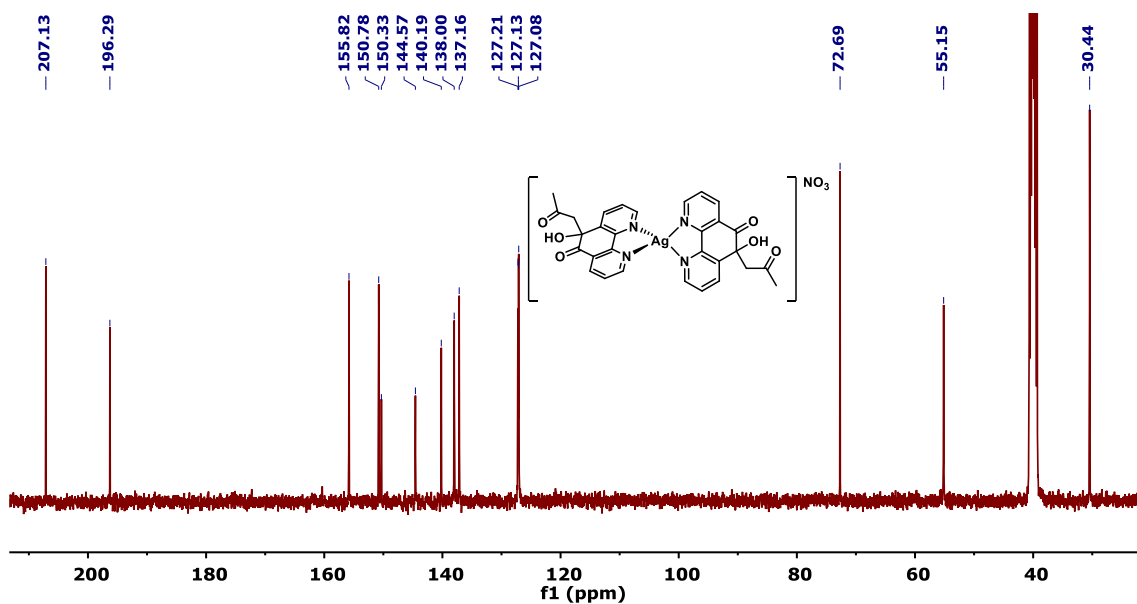


Figure S11. ^{13}C -NMR of **2Ag** ($DMSO_d_6$, 298 K)

$[Ag(4,5\text{-diazafuoren-9-one})_2]NO_3$ (**3Ag**)

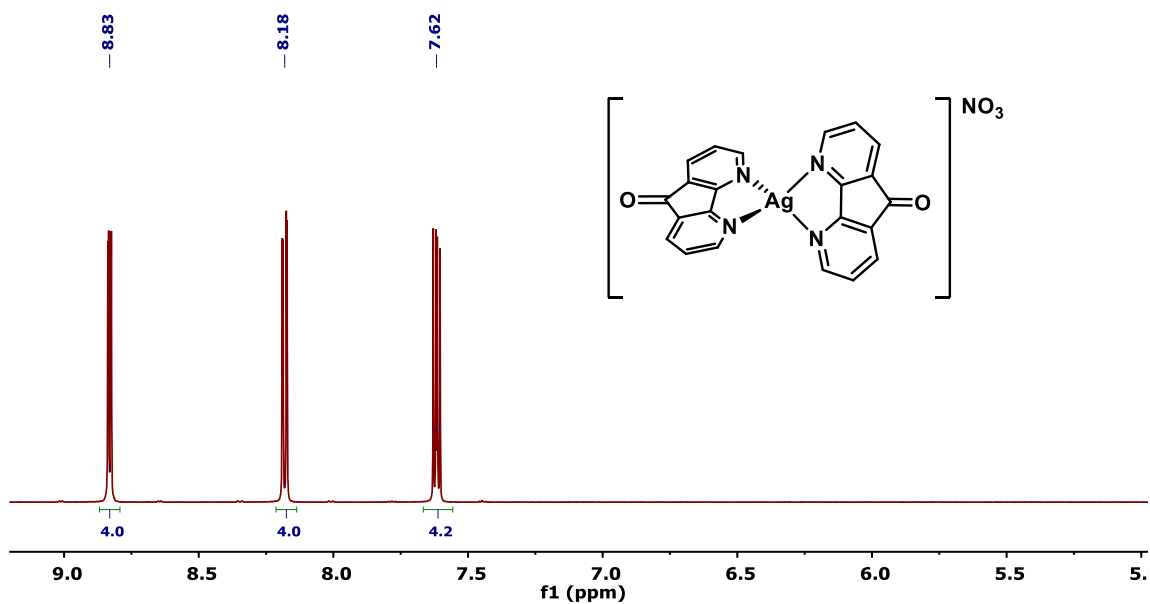


Figure S12. 1H -NMR of **3Ag** ($DMSO_d_6$, 298 K)

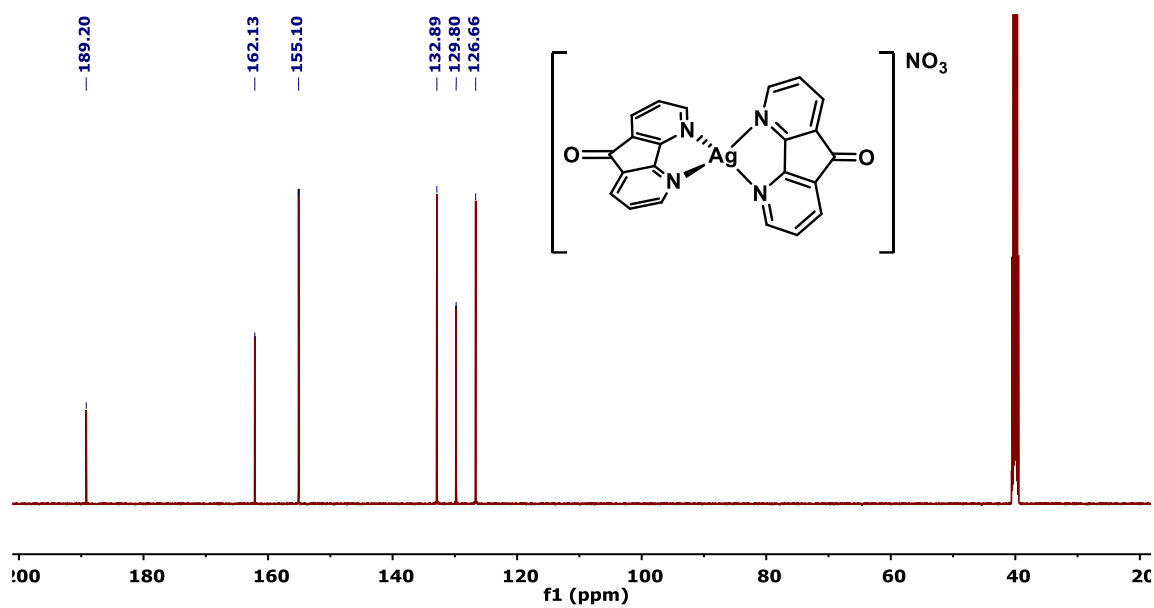


Figure S13. ^{13}C -NMR of **3Ag** (DMSO_d_6 , 298 K)

[Ag(9-hydroxy-9-(2-oxypropyl)-4,5-diazafluorene) $_2$] NO_3 (**4Ag**)

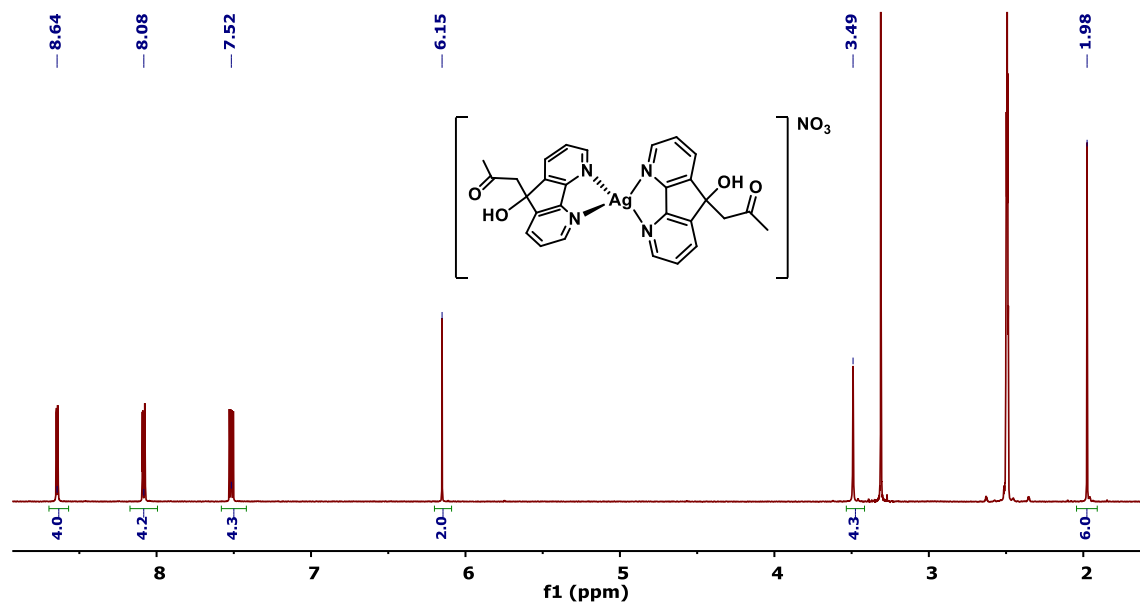


Figure S14. ^1H -NMR of **4Ag** (DMSO_d_6 , 298 K)

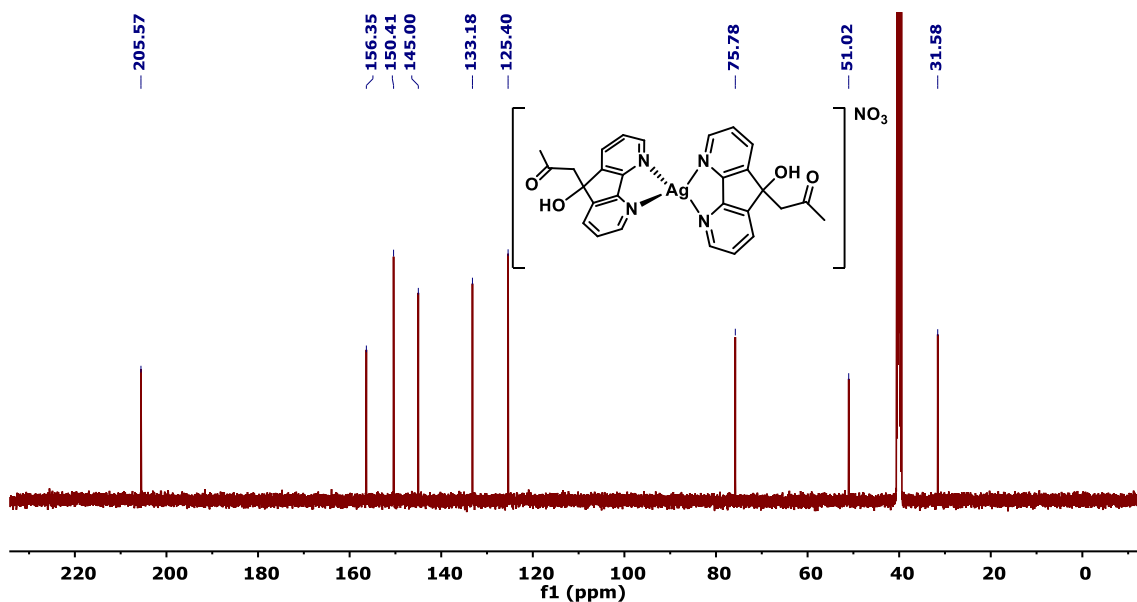


Figure S15. ^{13}C -NMR of **4Ag** (DMSO_d_6 , 298 K)

3. Pt(II) Complexes: NMR spectra

$[\text{Pt}(\text{C}_6\text{F}_5)_2(1,10\text{-phenanthroline-5,6-dione})]$ (**1Pt**):

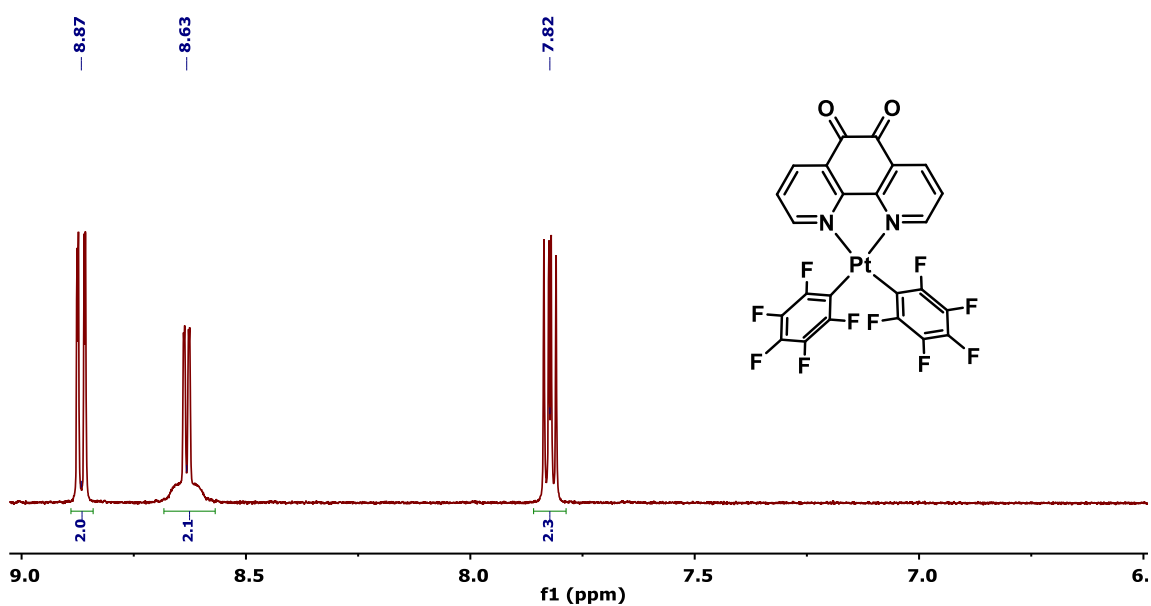


Figure S16. ^1H -NMR of **1Pt** (CD_2Cl_2 , 298 K)

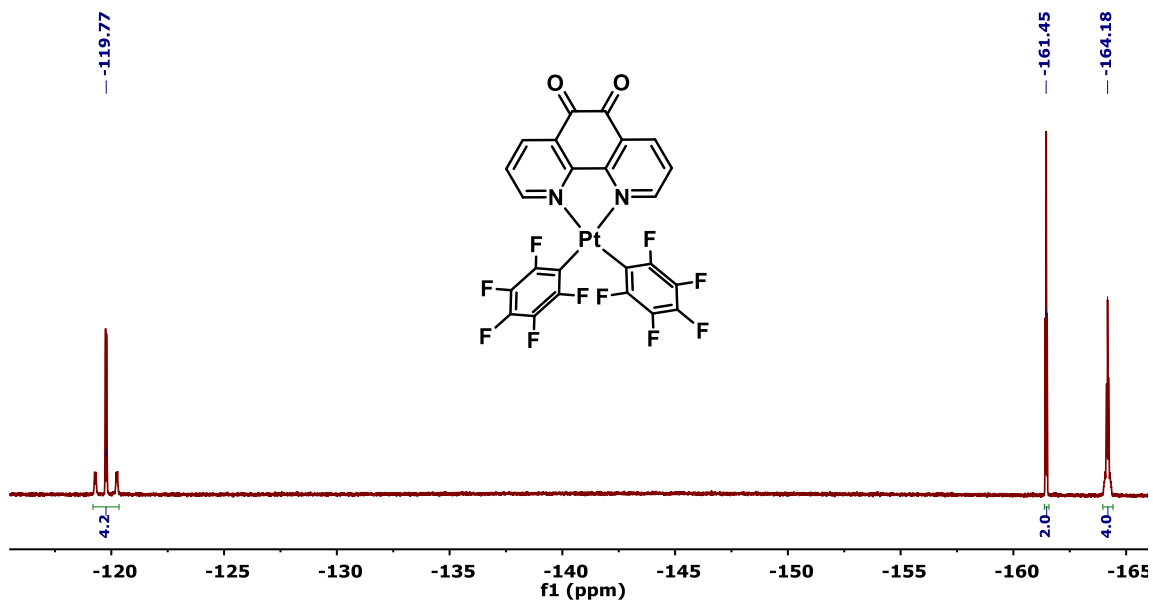


Figure S17. ^{19}F -NMR of **1Pt** (CD_2Cl_2 , 298 K)

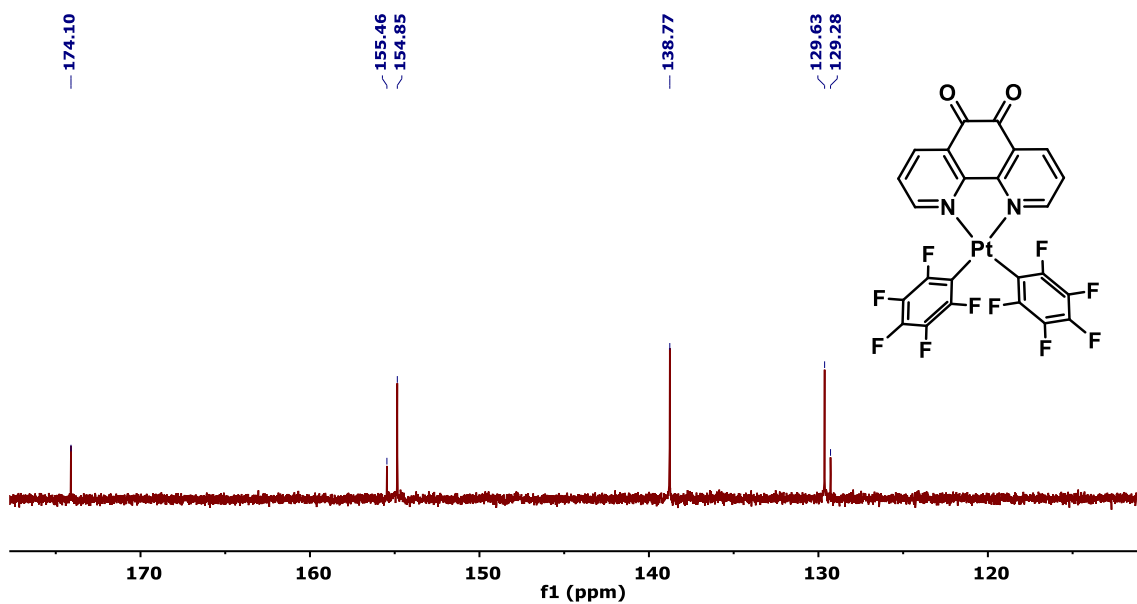


Figure S18. ^{13}C -NMR of **1Pt** (CD_2Cl_2 , 298 K)

[Pt(C₆F₅)₂((R/S)-6-hydroxy-6-(2-oxypropyl)-1,10-phenanthroline-5(6H)-one)] (**2Pt**):

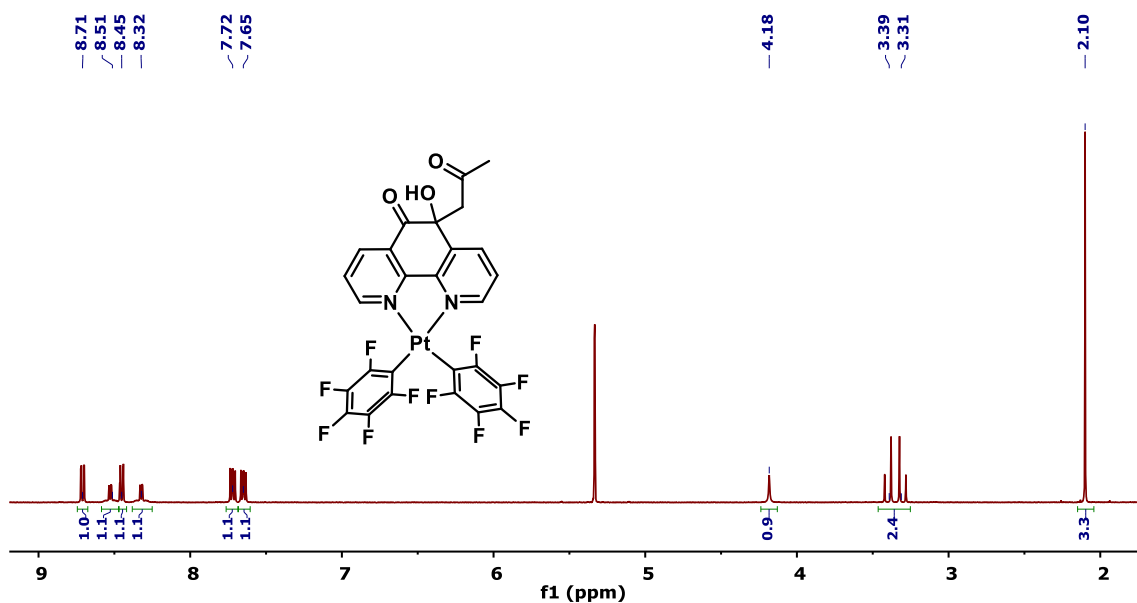


Figure S19. ¹H-NMR of **2Pt** (CD₂Cl₂, 298 K)

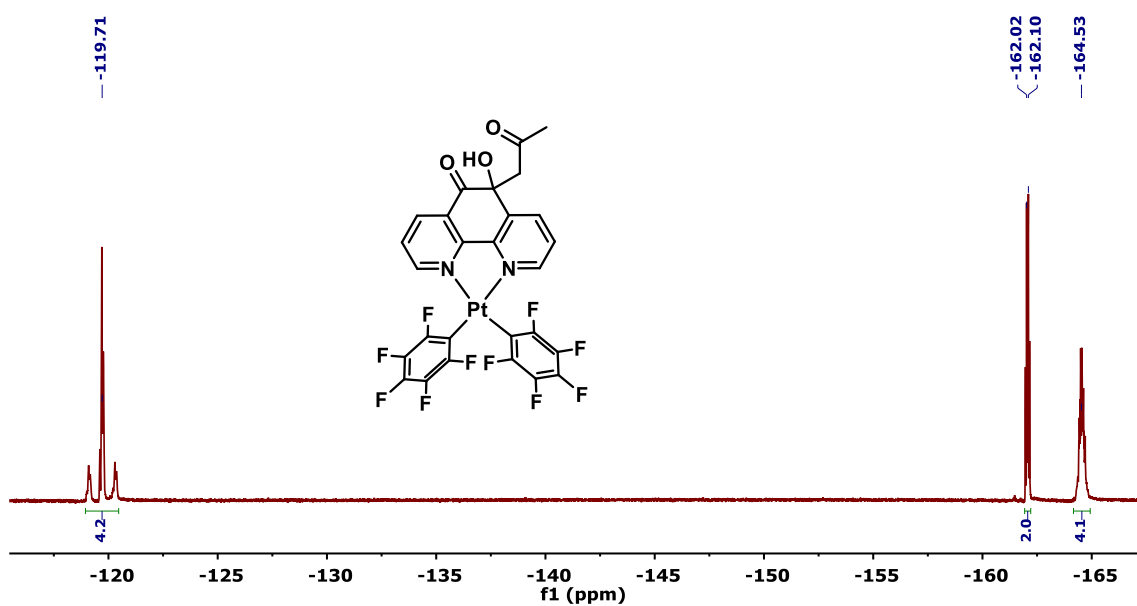


Figure S20. ¹⁹F-NMR of **2Pt** (CD₂Cl₂, 298 K)

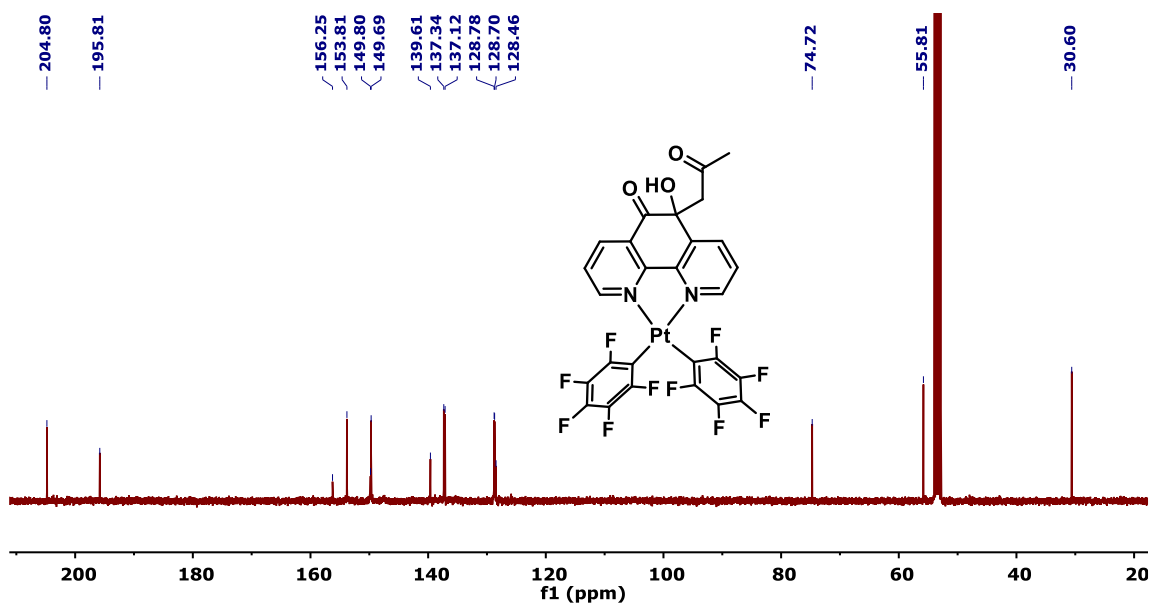


Figure S21. ^{13}C -NMR of **2Pt** (CD_2Cl_2 , 298 K)

[$\text{Pt}(\text{C}_6\text{F}_5)_2(4,5\text{-diazafuoren-9-one)}$] (**3Pt**):

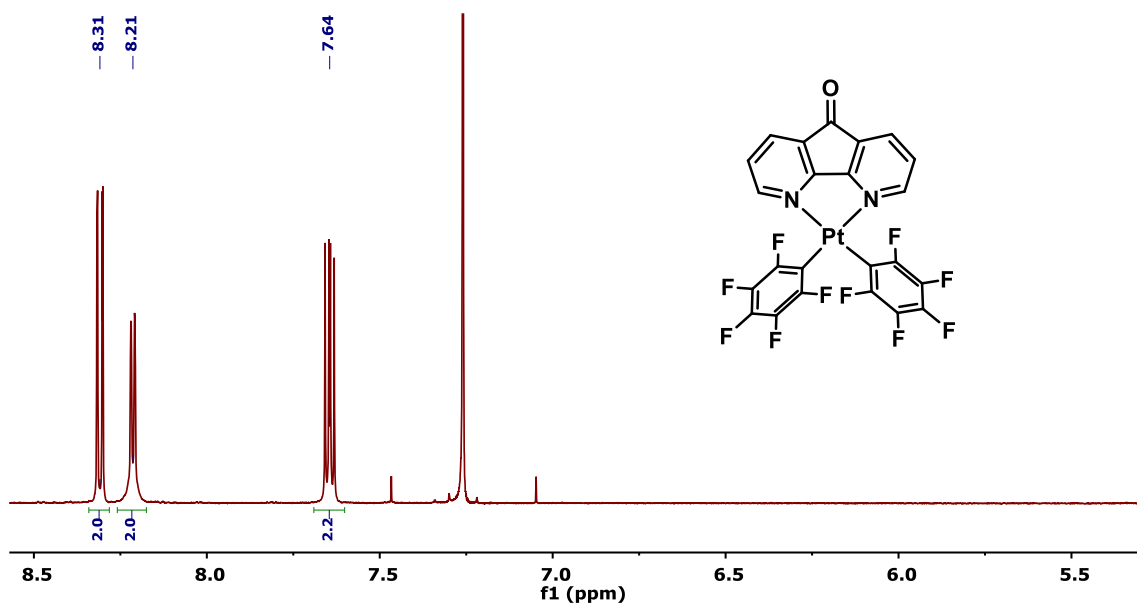
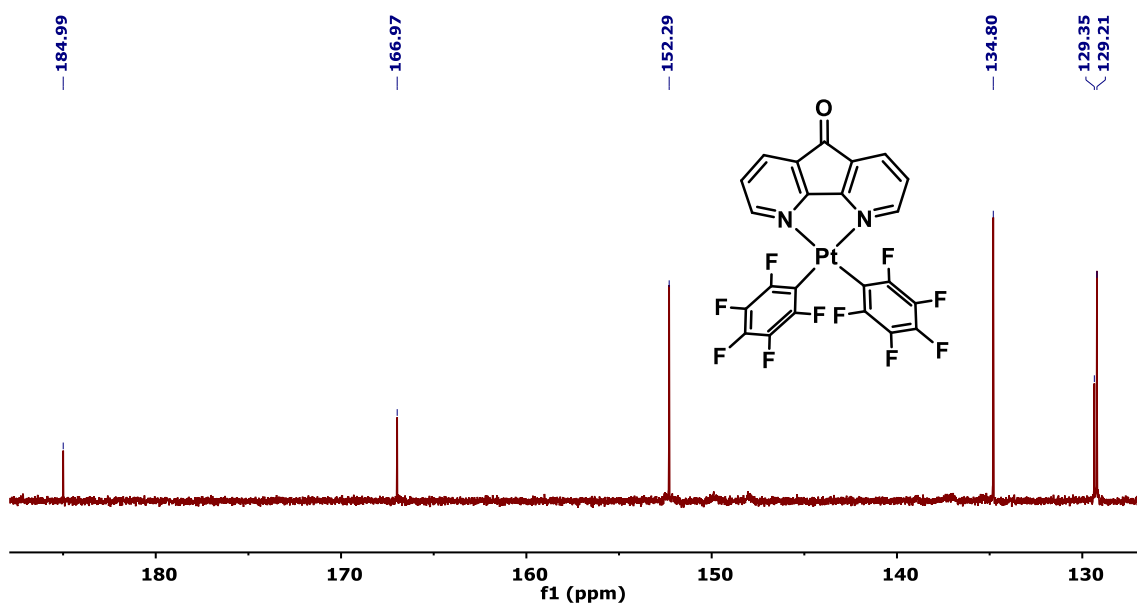
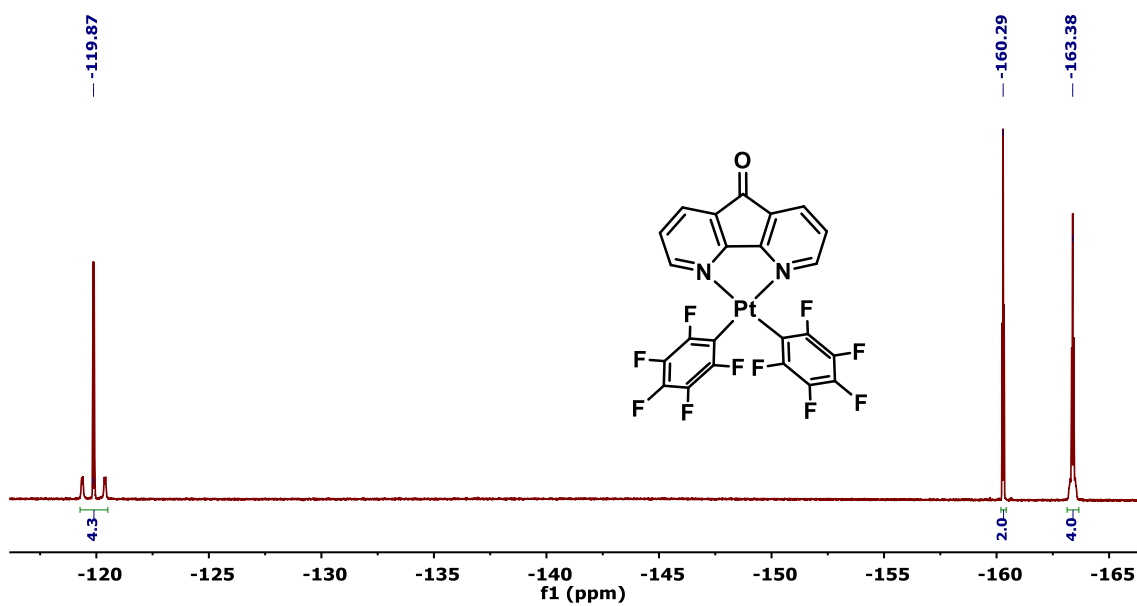


Figure S22. ^1H -NMR of **3Pt** (CDCl_3 , 298 K)



[Pt(C₆F₅)₂(9-hydroxy-9-(2-oxopropyl)-4,5-diazafluorene)] (**4Pt**):

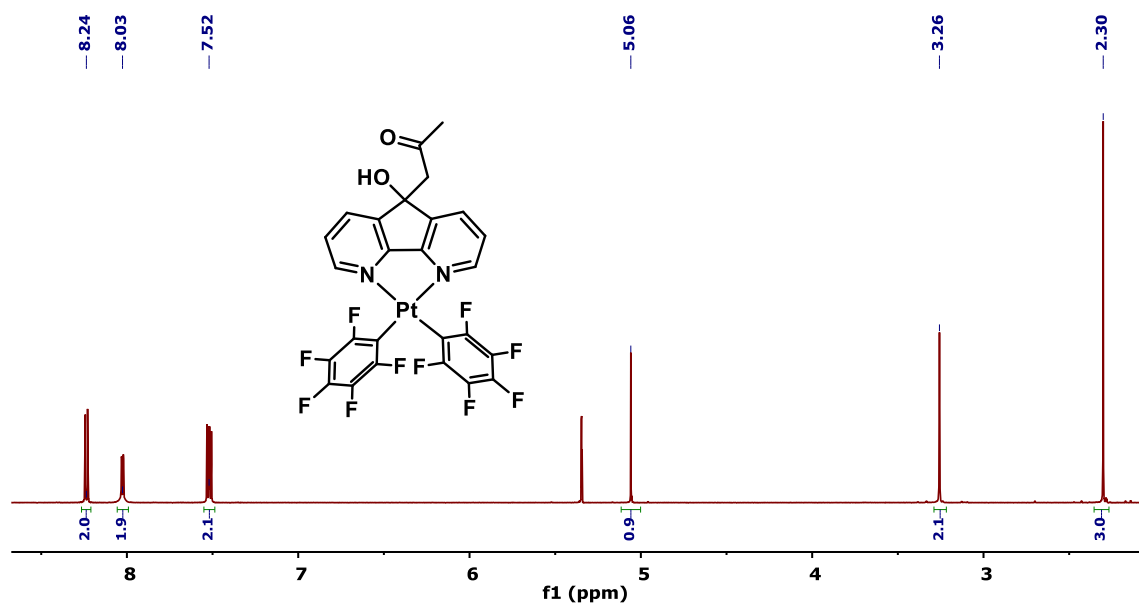


Figure S25. ¹H-NMR of **4Pt** (CD₂Cl₂, 298 K)

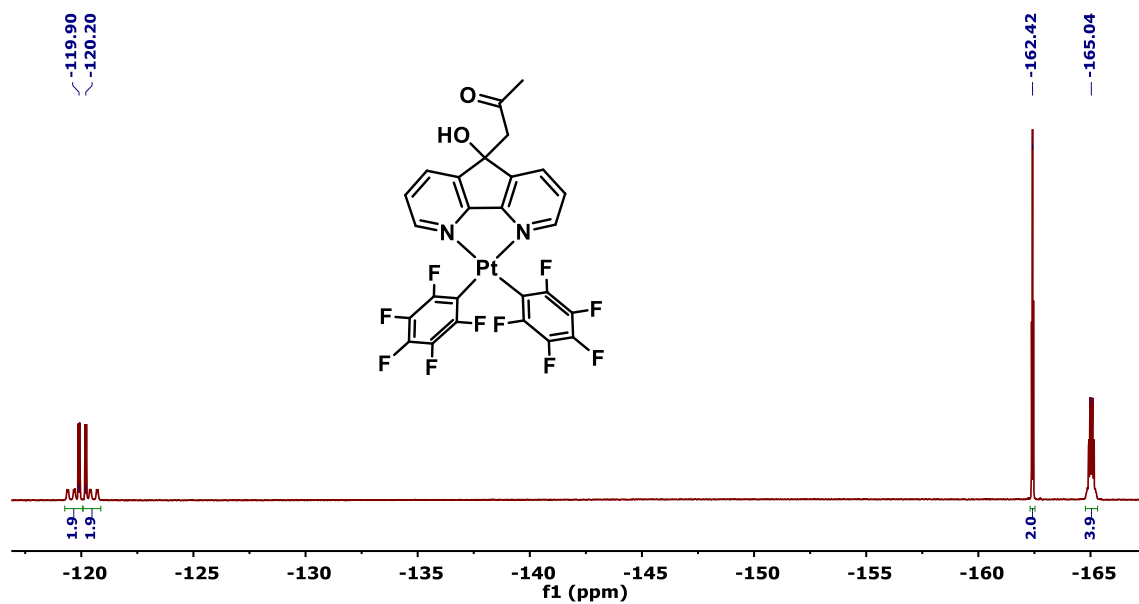


Figure S26. ¹⁹F-NMR of **4Pt** (CD₂Cl₂, 298 K)

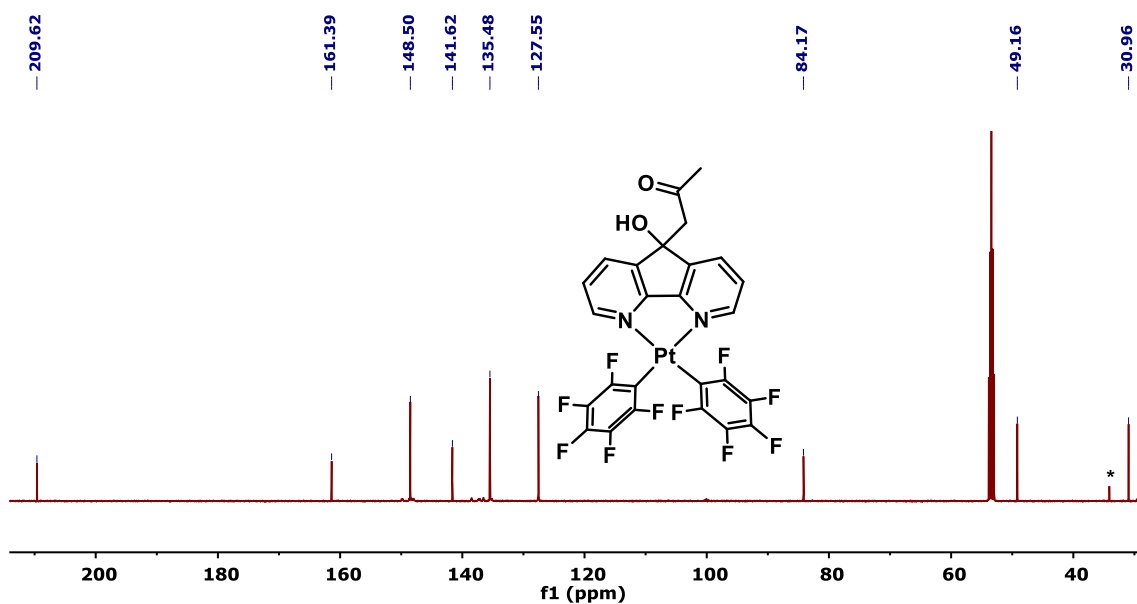


Figure S27. ^{13}C -NMR of **4Pt** (CD_2Cl_2 , 298 K). *Signal corresponding to n-pentane

4. ESI-TOF mass spectra of **2Ag**

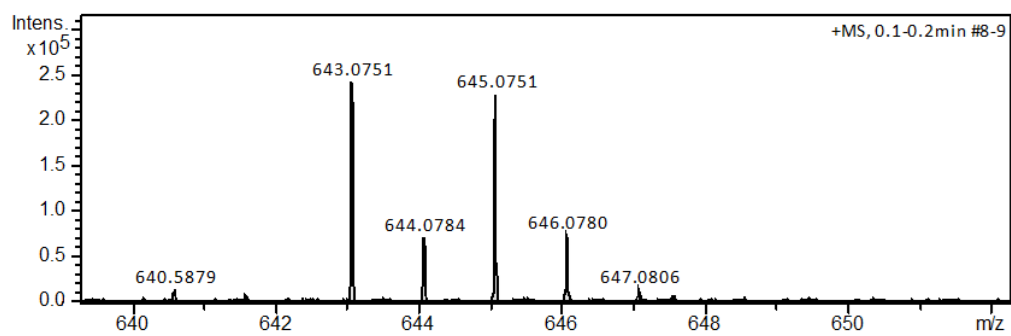


Figure S28. ESI-TOF mass spectra of **2Ag** between m/z 639 and 652, where the characteristic peak doublet of silver mononuclear species is observed.

5. Stability of the complexes in DMSO

Stability of $[\text{Ag}((R/S)\text{-6-hydroxy-6-(2-oxypropyl)-1,10-phenanthroline-5(6H)-one)}_2]\text{NO}_3$ (**2Ag**) in DMSO:

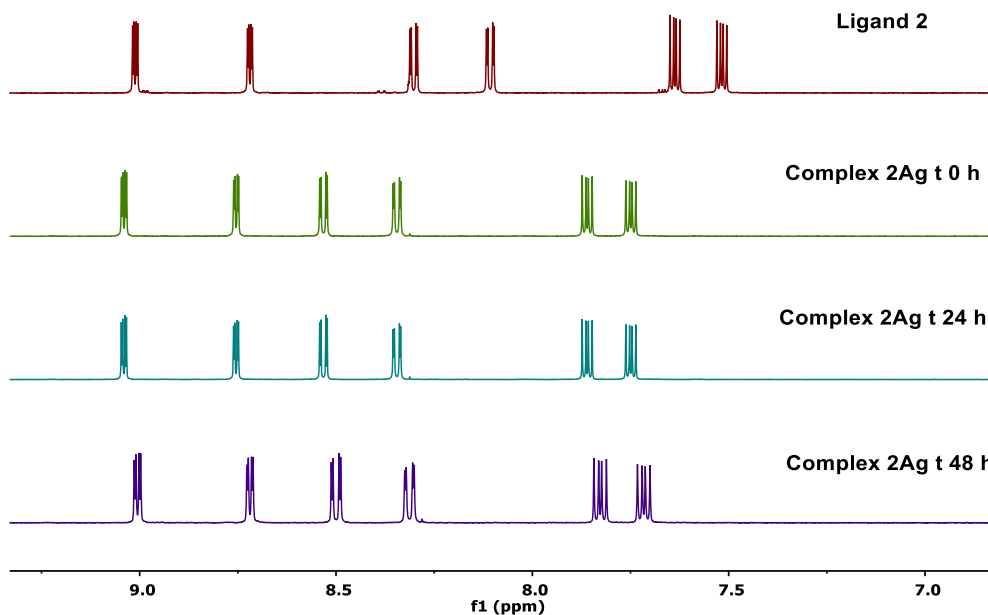


Figure S29. Comparison of the aromatic zone of the $^1\text{H-NMR}$ spectra of **2Ag** 5 mM in DMSO-d_6 over time vs ligand **2**

Stability of $[\text{Ag}(9\text{-hydroxy-9-(2-oxypropyl)-4,5-diazafluorene)}_2]\text{NO}_3$ (**4Ag**) in DMSO:

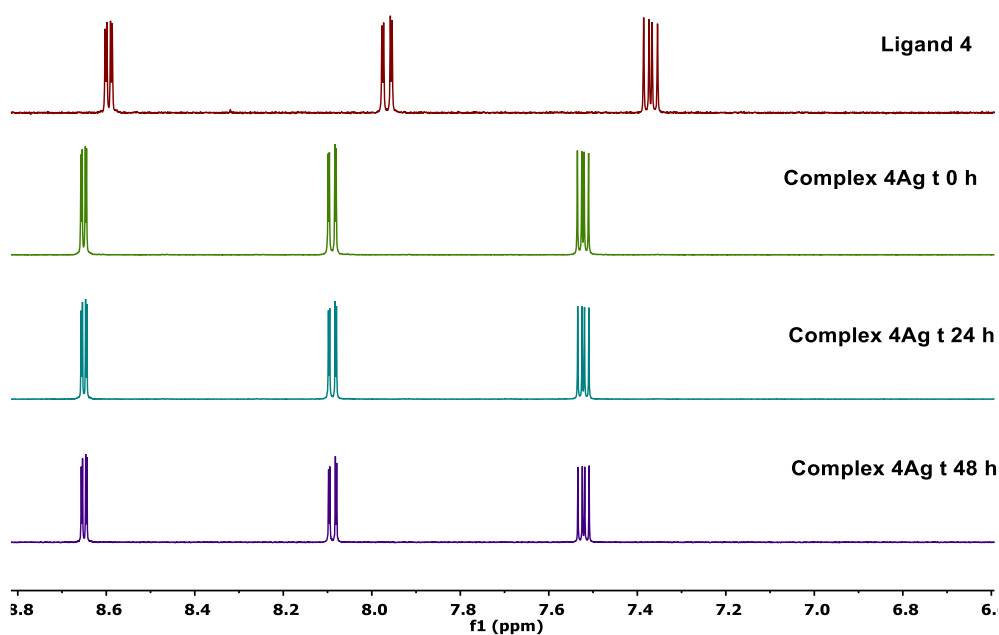


Figure S30. Comparison of the aromatic zone of the $^1\text{H-NMR}$ spectra of **4Ag** 5 mM in DMSO-d_6 over time vs ligand **4**

Stability of [Pt(C₆F₅)₂(9-hydroxy-9-(2-oxypropyl)-4,5-diazafluorene)] (4Pt) in DMSO:

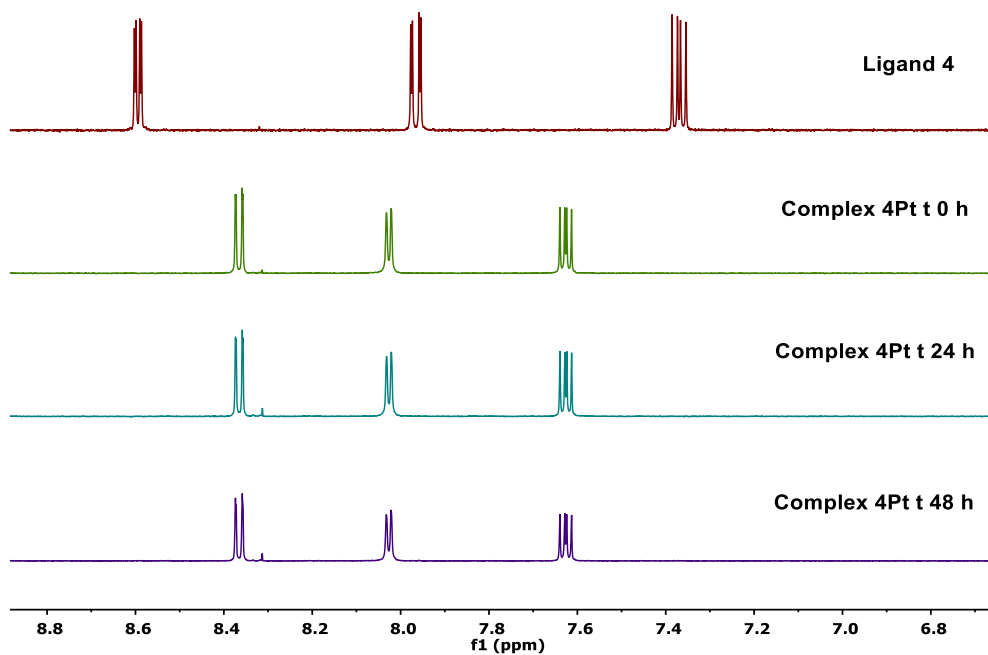


Figure S31. Comparison of the aromatic zone of the ¹H-NMR spectra of **4Pt** 5 mM in DMSO_d₆ over time vs ligand **4**

Stability of [Pt(C₆F₅)₂(4,5-diazafluoren-9-one)] (3Pt) in DMSO:

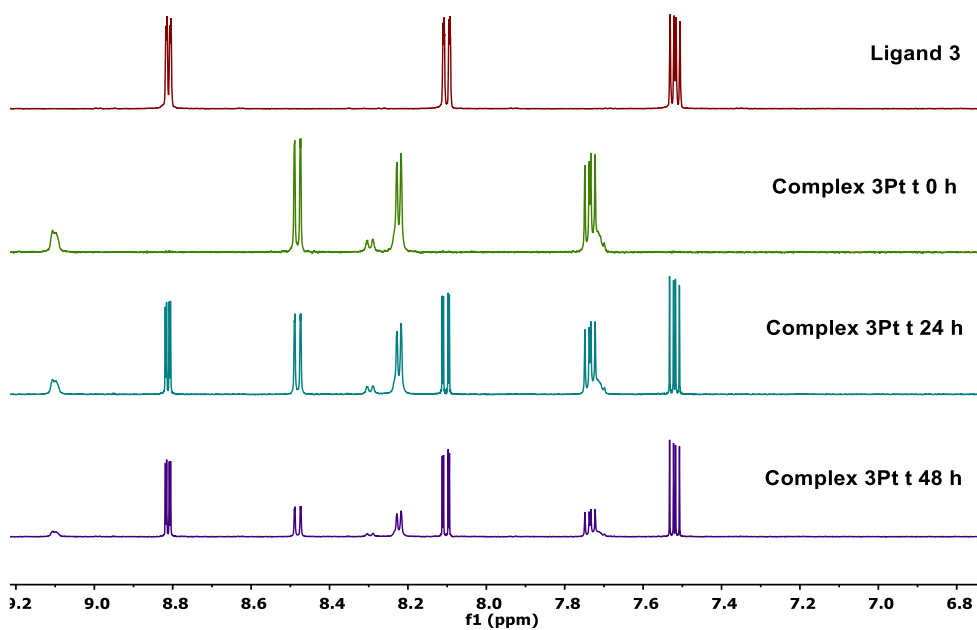


Figure S32. Comparison of the aromatic zone of the ¹H-NMR spectra of **3Pt** 5 mM in DMSO_d₆ over time vs ligand **3**

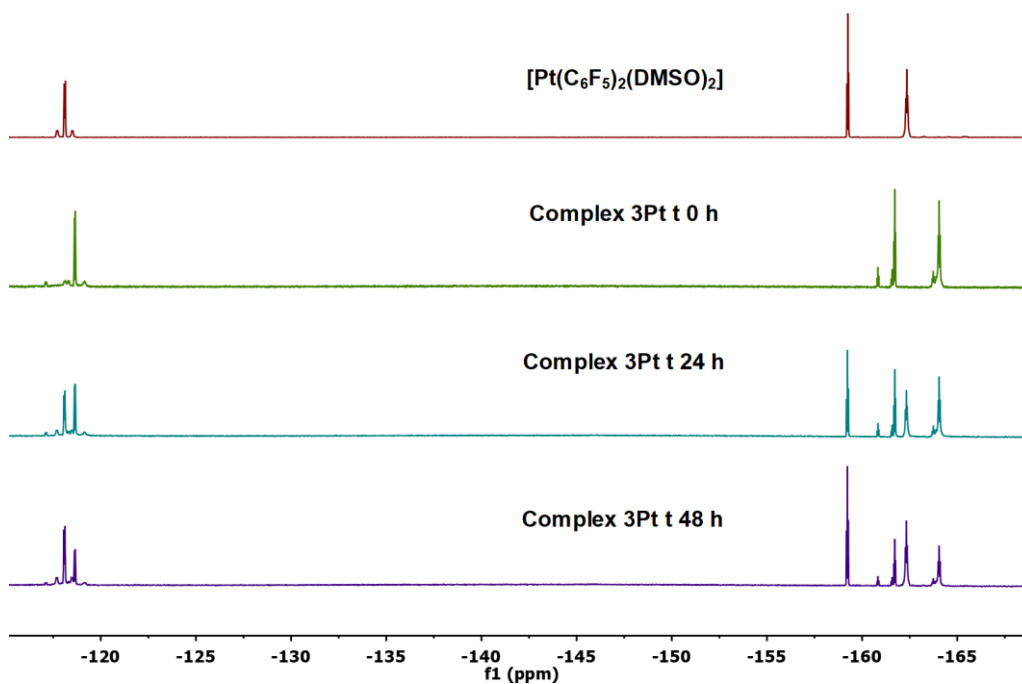


Figure S33. Comparison of the ^{19}F -NMR spectra of **3Pt** 5 mM in $\text{DMSO}d_6$ over time vs $[\text{Pt}(\text{C}_6\text{F}_5)_2(\text{DMSO})_2]$

6. Stability of the compounds in $\text{DMSO}:\text{H}_2\text{O}$ (3:1)

Stability of $[\text{Ag}(\text{9-hydroxy-9-(2-oxypropyl)-4,5-diazafluorene})_2]\text{NO}_3$ (**4Ag**) in $\text{DMSO}:\text{H}_2\text{O}$ (3:1)

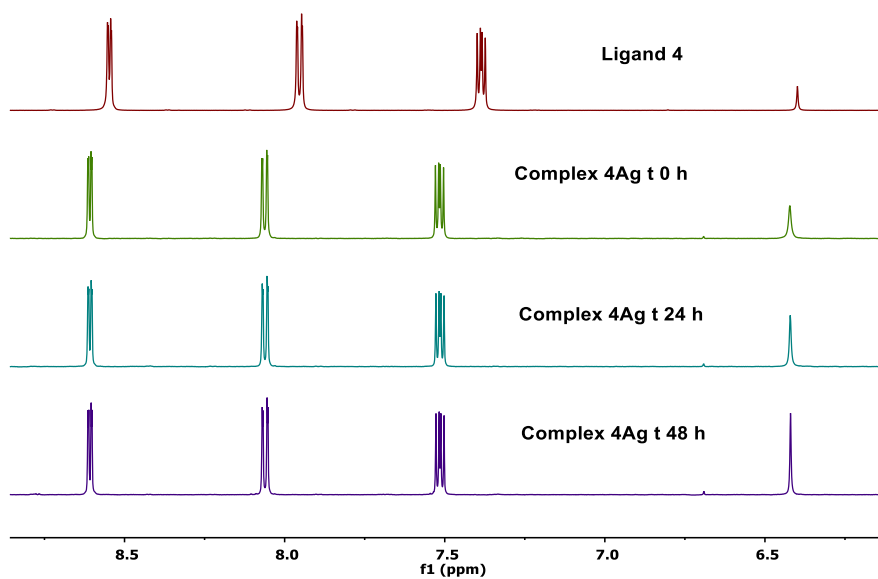


Figure S34. Comparison of the aromatic zone of the ^1H -NMR spectra of **4Ag** 2.5 mM in $\text{DMSO}d_6:\text{H}_2\text{O}$ (3:1) over time vs ligand **4**

Stability of $[\text{Pt}(\text{C}_6\text{F}_5)_2((R/S)\text{-6-hydroxy-6-(2-oxypropyl)-1,10-phenanthroline-5(6H)-one})]$ (**2Pt**) in $\text{DMSO}:\text{H}_2\text{O}$ (3:1)

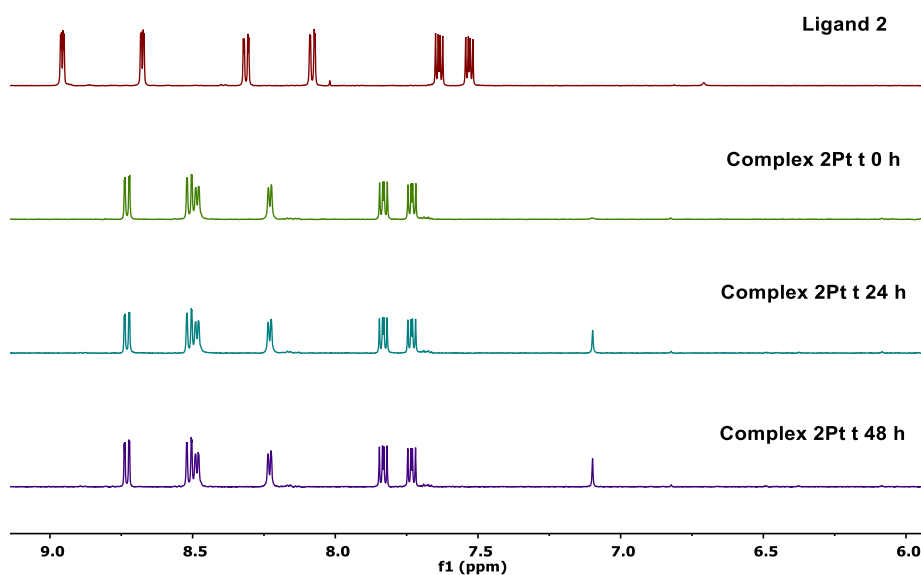


Figure S35. Comparison of the aromatic zone of the $^1\text{H-NMR}$ spectra of **2Pt** 2.5 mM in $\text{DMSO}_d_6:\text{H}_2\text{O}$ (3:1) over time vs ligand 2

Stability of $[\text{Pt}(\text{C}_6\text{F}_5)_2(4,5\text{-diazafuoren-9-one})]$ (**3Pt**) in $\text{DMSO}:\text{H}_2\text{O}$ (3:1):

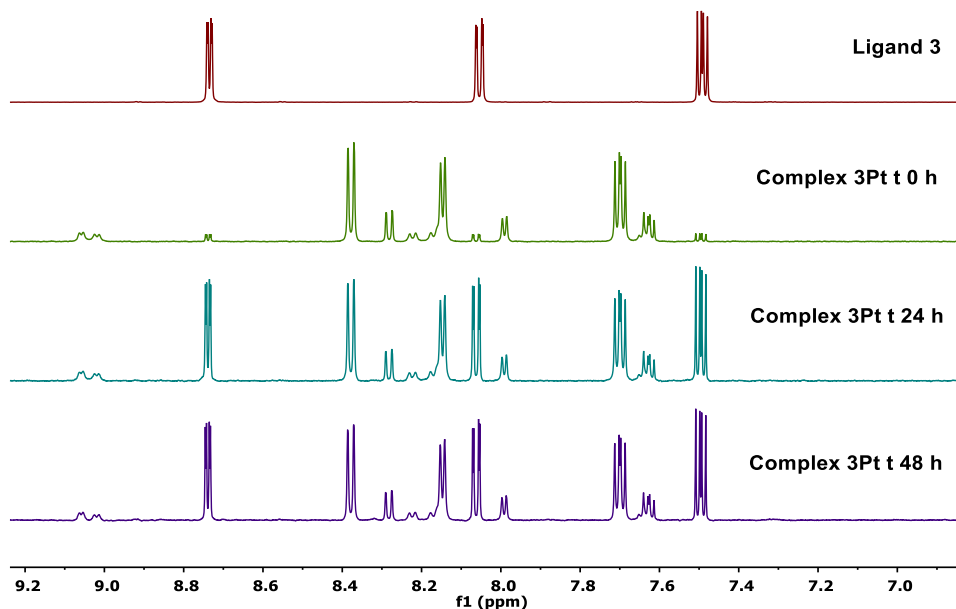


Figure S36. Comparison of the aromatic zone of the $^1\text{H-NMR}$ spectra of **3Pt** 2.5 mM in $\text{DMSO}_d_6:\text{H}_2\text{O}$ (3:1) over time vs ligand 3

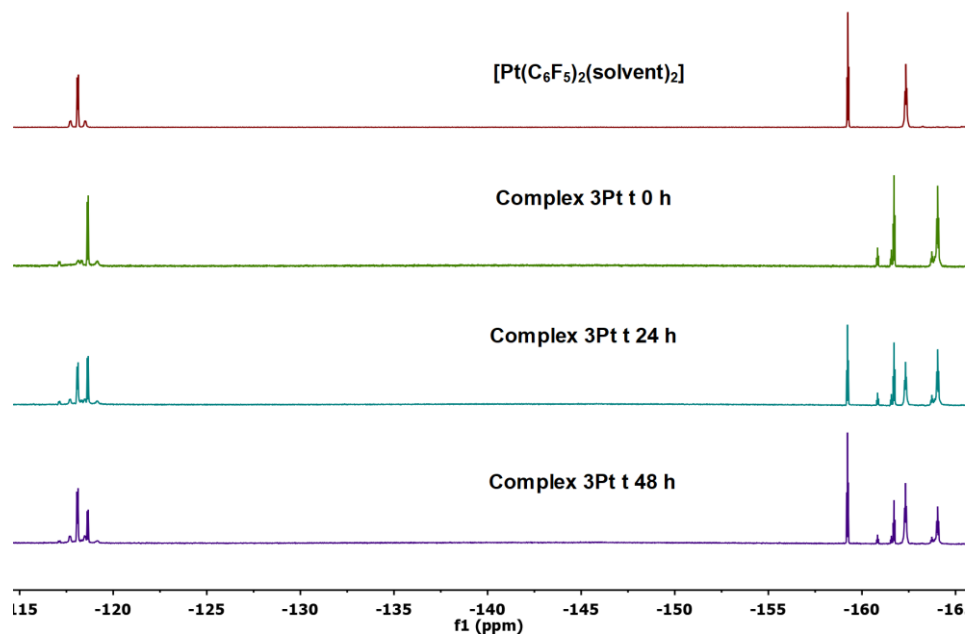


Figure S37. Comparison of the ^{19}F -NMR spectra of **3Pt** 2.5 mM in $\text{DMSO}_d_6:\text{H}_2\text{O}$ (3:1) over time vs $[\text{Pt}(\text{C}_6\text{F}_5)_2(\text{solvent})_2]$

Stability of $[\text{Ag}(\text{1,10-phenanthroline-5,6-dione})_2]\text{NO}_3$ (**1Ag**) in $\text{DMSO}:\text{H}_2\text{O}$ (3:1)

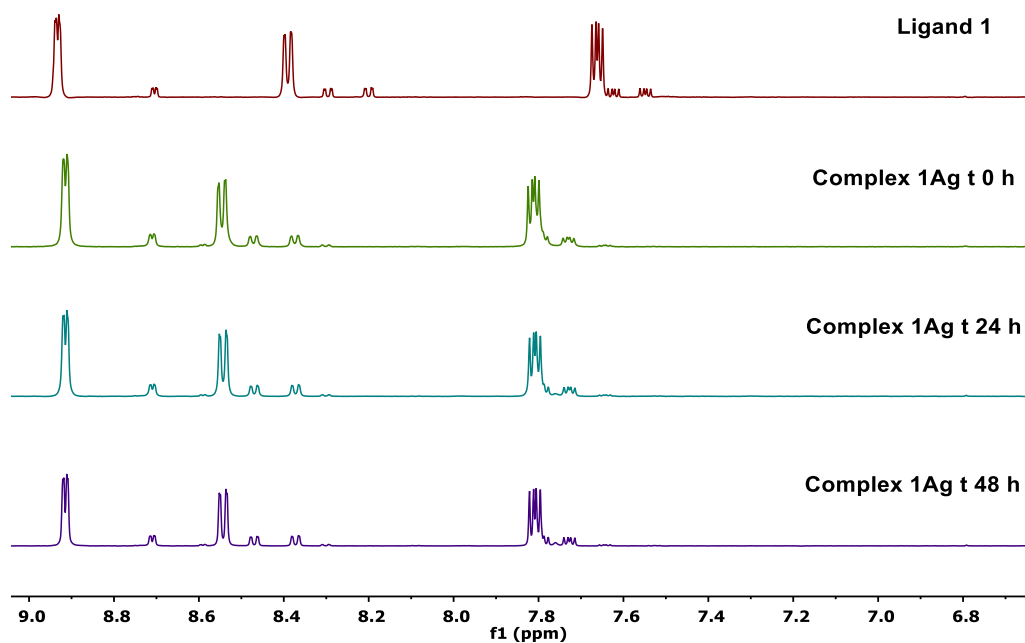


Figure S38. Comparison of the aromatic zone of the ^1H -NMR spectra of **1Ag** 2.5 mM in $\text{DMSO}_d_6:\text{H}_2\text{O}$ (3:1) over time vs ligand **1**

Stability of $[\text{Pt}(\text{C}_6\text{F}_5)_2(1,10\text{-phenanthroline-5,6\text{-dione})}]$ (**1Pt**) in $\text{DMSO}:\text{H}_2\text{O}$ (3:1):

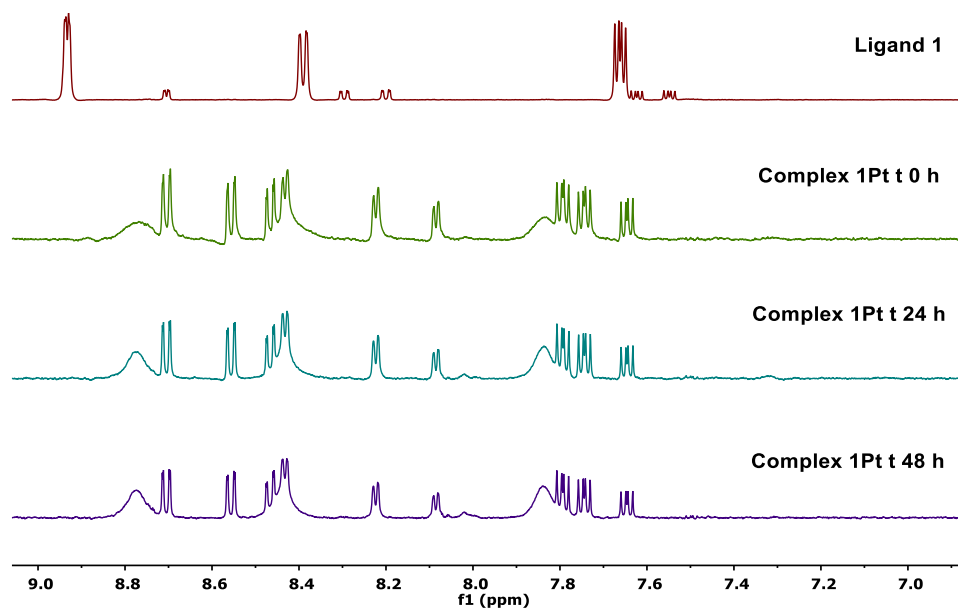


Figure S39. Comparison of the aromatic zone of the $^1\text{H-NMR}$ spectra of **1Pt** 2.5 mM in $\text{DMSO}_d_6:\text{H}_2\text{O}$ (3:1) over time vs ligand **1**

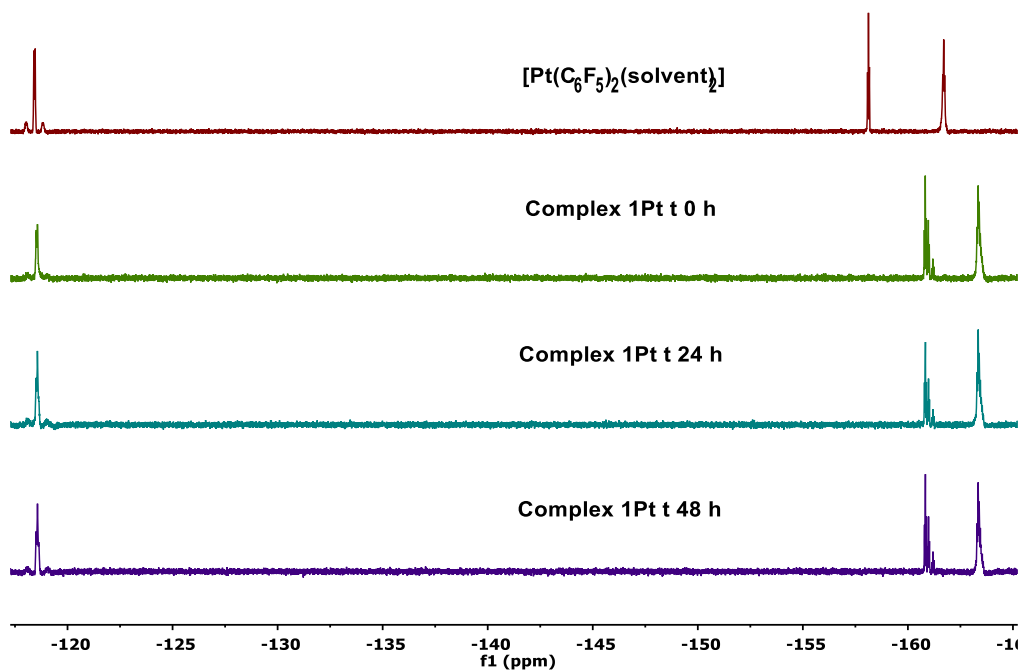


Figure S40. Comparison of the $^{19}\text{F-NMR}$ spectra of **1Pt** 2.5 mM in $\text{DMSO}_d_6:\text{H}_2\text{O}$ (3:1) over time vs $[\text{Pt}(\text{C}_6\text{F}_5)_2(\text{solvent})_2]$

7. Crystal data and structural refinement results

(R/S)-6-hidroxy-6-(2-oxypropyl)-1,10-phenanthroline-5(6H)-one (**2**)

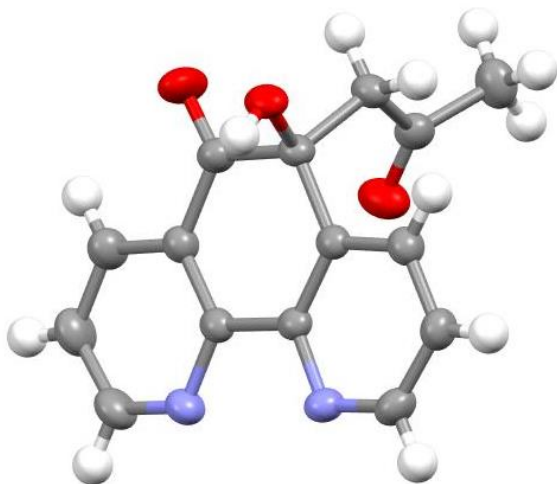


Figure S41. Single-crystal X-ray structure of **2**

Table S1. Crystallographic data of compound 2	
Compound	2
Empirical formula	C ₁₅ H ₁₂ N ₂ O ₃
Formula weight	268.27
Temperature/K	298.9(6)
Crystal system	monoclinic
Space group	P2 ₁ /c
a/Å	11.2848(4)
b/Å	12.7019(3)
c/Å	9.0158(3)
α/°	90
β/°	106.313(4)
γ/°	90
Volume/Å ³	1240.28(7)
Z	4
ρ _{calc} /cm ³	1.437
μ/mm ⁻¹	0.843
F(000)	560.0
Crystal size/mm ³	0.26 × 0.227 × 0.082
Radiation	Cu Kα (λ = 1.54184)
2θ range for data collection/°	8.164 to 150.142
Index ranges	-13 ≤ h ≤ 14, -15 ≤ k ≤ 9, -11 ≤ l ≤ 10
Reflections collected	7077
Independent reflections	2515 [R _{int} = 0.0248, R _{sigma} = 0.0228]
Data/restraints/parameters	2515/0/183
Goodness-of-fit on F ²	1.054
Final R indexes [I >= 2σ(I)]	R ₁ = 0.0401, wR ₂ = 0.1088
Final R indexes [all data]	R ₁ = 0.0522, wR ₂ = 0.1202
Largest diff. peak/hole / e Å ⁻³	0.19/-0.17

9-hidroxy-9-(2-oxypropyl)-4,5-diazafluorene (**4**)

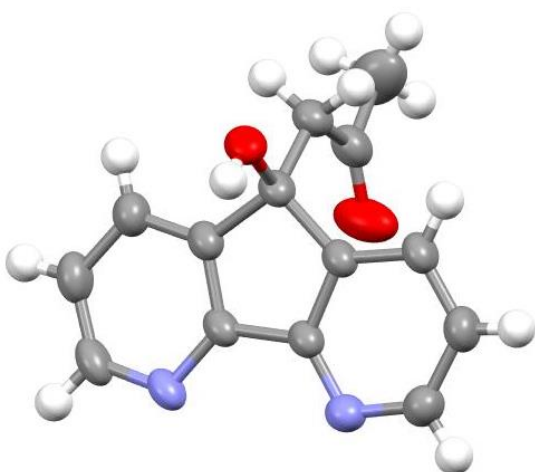


Figure S42. Single-crystal X-ray structure of **4**

Table S2. Crystallographic data of compound 4	
Compound	4
Empirical formula	C ₁₄ H ₁₂ N ₂ O ₂
Formula weight	240.26
Temperature/K	293
Crystal system	monoclinic
Space group	P2 ₁ /c
a/Å	9.6279(3)
b/Å	11.2671(3)
c/Å	11.9805(5)
α/°	90
β/°	111.451(4)
γ/°	90
Volume/Å ³	1209.60(8)
Z	4
ρ _{calc} /cm ³	1.319
μ/mm ⁻¹	0.734
F(000)	504.0
Crystal size/mm ³	0.585 × 0.264 × 0.161
Radiation	Cu Kα (λ = 1.54184)
2θ range for data collection/°	9.87 to 140.778
Index ranges	-11 ≤ h ≤ 10, -13 ≤ k ≤ 12, -13 ≤ l ≤ 14
Reflections collected	7144
Independent reflections	2276 [R _{int} = 0.0201, R _{sigma} = 0.0160]
Data/restraints/parameters	2276/0/165
Goodness-of-fit on F ²	1.029
Final R indexes [I >= 2σ(I)]	R ₁ = 0.0431, wR ₂ = 0.1163
Final R indexes [all data]	R ₁ = 0.0537, wR ₂ = 0.1270
Largest diff. peak/hole / e Å ⁻³	0.20/-0.19

[Ag(1,10-phenanthroline-5,6-dione)₂](NO₃) (**1Ag**)

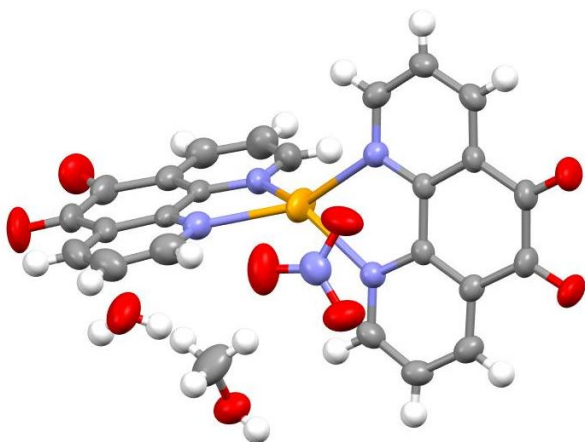


Figure S43. Single-crystal X-ray structure of **1Ag**

Table S3. Crystallographic data of compound 1Ag	
Compound	1Ag.H₂O.CH₃OH
Empirical formula	C ₂₅ H ₁₈ AgN ₅ O ₉
Formula weight	640.31
Temperature/K	293
Crystal system	monoclinic
Space group	P2 ₁ /n
a/Å	8.7751(6)
b/Å	25.6195(11)
c/Å	10.8341(9)
α/°	90
β/°	93.284(7)
γ/°	90
Volume/Å ³	2431.7(3)
Z	4
ρ _{calc} /cm ³	1.749
μ/mm ⁻¹	0.896
F(000)	1288.0
Crystal size/mm ³	0.284 × 0.1 × 0.07
Radiation	Mo Kα (λ = 0.71073)
2θ range for data collection/°	6.628 to 59.358
Index ranges	-11 ≤ h ≤ 11, -32 ≤ k ≤ 35, -14 ≤ l ≤ 10
Reflections collected	16863
Independent reflections	5927 [R _{int} = 0.0346, R _{sigma} = 0.0481]
Data/restraints/parameters	5927/0/366
Goodness-of-fit on F ²	1.021
Final R indexes [I >= 2σ (I)]	R ₁ = 0.0522, wR ₂ = 0.1138
Final R indexes [all data]	R ₁ = 0.1071, wR ₂ = 0.1401
Largest diff. peak/hole / e Å ⁻³	0.53/-0.75

[Ag(4,5-diazafluoren-9-one)₂](NO₃) (**3Ag**)

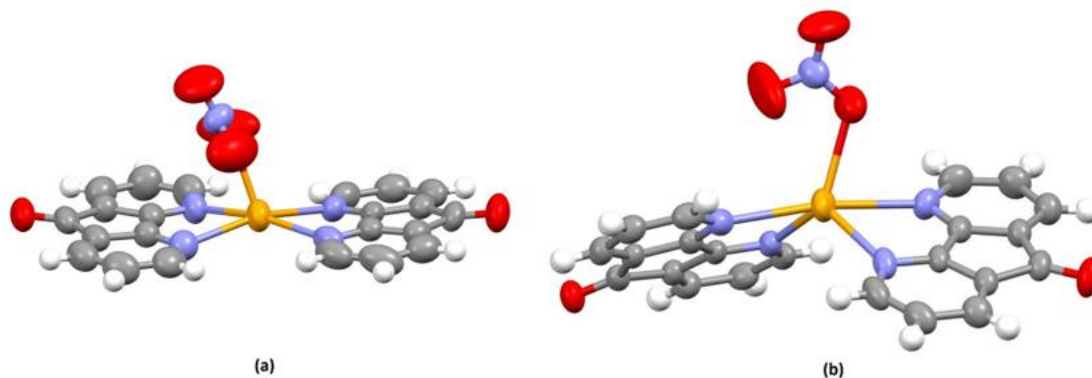


Figure S44. Single-crystal X-ray structure of **3Ag**. (a) polymorph A. (b) polymorph B

[Ag(4,5-diazafluoren-9-one)₂]₂NO₃ (**3Ag**)-Cristal structure of polymorph A

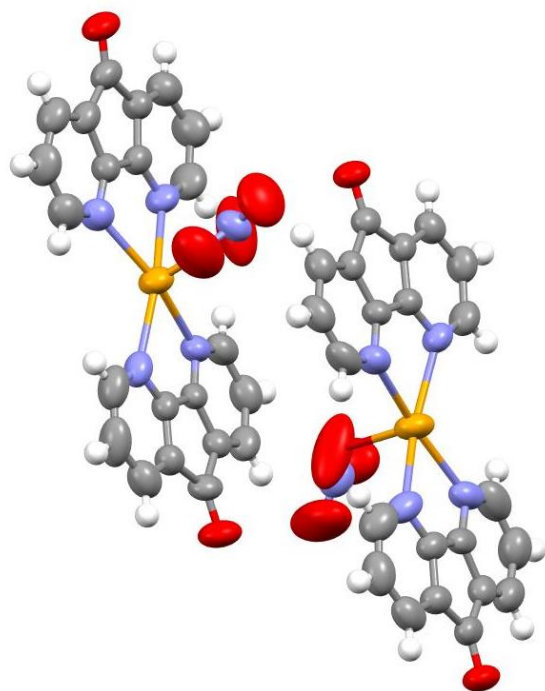


Figure S45. Single-crystal X-ray structure of **3Ag** (structure A)

Table S4. Crystallographic data of compound 3Ag polymorph A	
Compound	3Ag
Empirical formula	C ₄₄ H ₂₄ Ag ₂ N ₁₀ O ₁₀
Formula weight	1068.47
Temperature/K	298.1(8)
Crystal system	monoclinic
Space group	P2 ₁ /n
a/Å	13.3402(10)
b/Å	17.3188(9)
c/Å	17.4206(10)
α/°	90
β/°	98.249(6)
γ/°	90
Volume/Å ³	3983.1(4)
Z	4
ρ _{calc} /cm ³	1.782
μ/mm ⁻¹	1.061
F(000)	2128.0
Crystal size/mm ³	0.272 × 0.202 × 0.127
Radiation	MoKα (λ = 0.71073)
2θ range for data collection/°	6.606 to 59.548
Index ranges	-13 ≤ h ≤ 16, -23 ≤ k ≤ 16, -23 ≤ l ≤ 17
Reflections collected	26093
Independent reflections	9579 [R _{int} = 0.0444, R _{sigma} = 0.0561]
Data/restraints/parameters	9579/0/595
Goodness-of-fit on F ²	0.986
Final R indexes [I >= 2σ (I)]	R ₁ = 0.0585, wR ₂ = 0.1481
Final R indexes [all data]	R ₁ = 0.1543, wR ₂ = 0.2025
Largest diff. peak/hole / e Å ⁻³	0.63/-0.59

[Ag(4,5-diazafluoren-9-one)₂]₂NO₃ (**3Ag**)-Cristal structure B

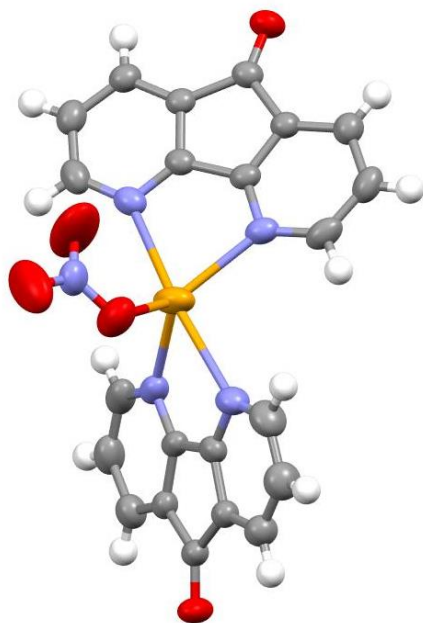


Figure S46. Single-crystal X-ray structure of **3Ag** (structure B)

Table S5. Crystallographic data of compound 3Ag polymorph B	
Compound	3Ag
Empirical formula	C ₂₂ H ₁₂ AgN ₅ O ₅
Formula weight	534.24
Temperature/K	293
Crystal system	triclinic
Space group	P-1
a/Å	8.0748(5)
b/Å	10.6080(8)
c/Å	12.7848(11)
α/°	70.915(7)
β/°	80.672(7)
γ/°	73.368(6)
Volume/Å ³	988.78(14)
Z	2
ρ _{calc} /cm ³	1.794
μ/mm ⁻¹	1.068
F(000)	532.0
Crystal size/mm ³	0.136 × 0.132 × 0.049
Radiation	MoKα (λ = 0.71073)
2θ range for data collection/°	6.764 to 58.928
Index ranges	-7 ≤ h ≤ 11, -14 ≤ k ≤ 14, -14 ≤ l ≤ 16
Reflections collected	7531
Independent reflections	4598 [R _{int} = 0.0236, R _{sigma} = 0.0506]
Data/restraints/parameters	4598/0/298
Goodness-of-fit on F ²	1.027
Final R indexes [I >= 2σ (I)]	R ₁ = 0.0456, wR ₂ = 0.0878
Final R indexes [all data]	R ₁ = 0.0921, wR ₂ = 0.1106
Largest diff. peak/hole / e Å ⁻³	0.30/-0.43

[Pt(C₆F₅)₂(1,10-phenanthroline-5,6-dione)] (**1Pt**):

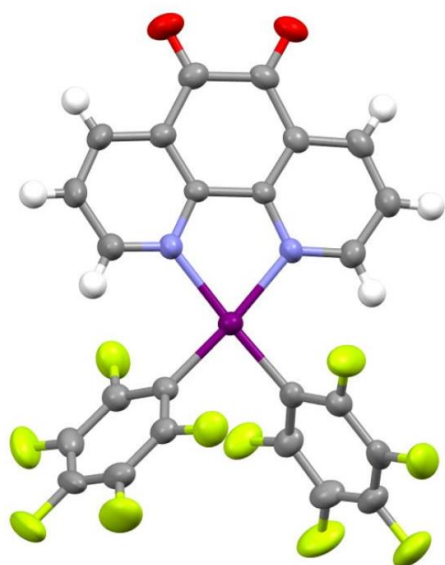


Figure S47. Single-crystal X-ray structure of **1Pt**

Table S6. Crystallographic data of compound 1Pt	
Compound	1Pt
Empirical formula	C ₂₄ H ₆ F ₁₀ N ₂ O ₂ Pt
Formula weight	739.40
Temperature/K	293
Crystal system	monoclinic
Space group	P2 ₁ /c
a/Å	13.2566(7)
b/Å	17.1842(8)
c/Å	10.4145(7)
α/°	90
β/°	111.555(6)
γ/°	90
Volume/Å ³	2206.5(2)
Z	4
ρ _{calc} /cm ³	2.226
μ/mm ⁻¹	6.471
F(000)	1392.0
Crystal size/mm ³	0.328 × 0.089 × 0.08
Radiation	MoKα (λ = 0.71073)
2θ range for data collection/°	6.668 to 59.444
Index ranges	-13 ≤ h ≤ 18, -16 ≤ k ≤ 21, -13 ≤ l ≤ 8
Reflections collected	11202
Independent reflections	5236 [R _{int} = 0.0292, R _{sigma} = 0.0488]
Data/restraints/parameters	5236/0/352
Goodness-of-fit on F ²	1.035
Final R indexes [I >= 2σ (I)]	R ₁ = 0.0339, wR ₂ = 0.0498
Final R indexes [all data]	R ₁ = 0.0582, wR ₂ = 0.0588
Largest diff. peak/hole / e Å ⁻³	0.78/-0.77

[Pt(C₆F₅)₂(4,5-diazafluoren-9-one)] (**3Pt**):

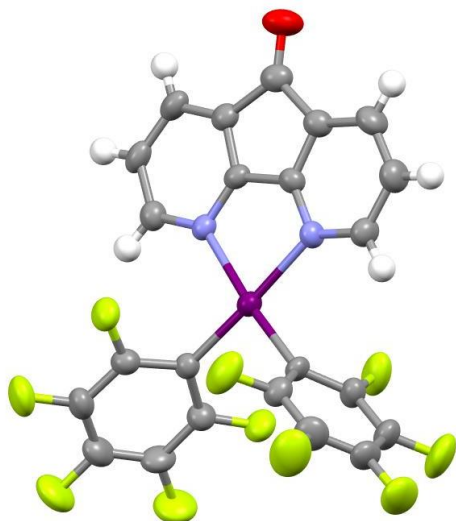


Figure S48. Single-crystal X-ray structure of **3Pt**

Table S7. Crystallographic data of compound 3Pt	
Compound	3Pt
Empirical formula	C ₂₃ H ₆ F ₁₀ N ₂ OPt
Formula weight	729.11
Temperature/K	293
Crystal system	triclinic
Space group	P-1
a/Å	8.5703(5)
b/Å	11.7050(7)
c/Å	12.8817(7)
α/°	81.523(5)
β/°	87.266(5)
γ/°	73.952(5)
Volume/Å ³	1228.27(13)
Z	2
ρ _{calc} /cm ³	1.971
μ/mm ⁻¹	5.861
F(000)	685.0
Crystal size/mm ³	0.311 × 0.088 × 0.086
Radiation	MoKα (λ = 0.71073)
2θ range for data collection/°	6.908 to 59.012
Index ranges	-11 ≤ h ≤ 11, -12 ≤ k ≤ 15, -16 ≤ l ≤ 15
Reflections collected	10209
Independent reflections	5746 [R _{int} = 0.0348, R _{sigma} = 0.0714]
Data/restraints/parameters	5746/0/334
Goodness-of-fit on F ²	0.932
Final R indexes [I >= 2σ (I)]	R ₁ = 0.0378, wR ₂ = 0.0515
Final R indexes [all data]	R ₁ = 0.0558, wR ₂ = 0.0593
Largest diff. peak/hole / e Å ⁻³	0.62/-0.67